◀ **Fig. 3** Quantified levels of glycolytic and TCA cycle intermediates (**a**) and phosphorylation levels of each phosphorylation site in associated enzymes (**b**) in normal (*left, open dots*) and tumor (*right, filled dots*) tissues obtained from lung and prostate cancer patients. *Encircled numbers* in (**a**) indicated next to the metabolic reactions involved in glycolysis and the TCA cycle correspond to the associated enzymes in (**b**). *Horizontal bars* represent mean ± SD of normal (*left*) and tumor (*right*) samples and each connected pair represents the values for the same patient. *Gray dots* represent the values for patients with non-SCC lung cancer (L4–L6, L8 and L9) and patients with moderately differentiated prostate cancer (P1 and P5–7). *N.D.* indicates that the metabolite level was below the detection limit of the analysis. *Asterisks* indicate the significant differences between normal and tumor tissue levels based on the Wilcoxon signed-rank test (*$p < 0.05$; **$p < 0.01$; and ***$p < 0.001$). *G6PI* glucose 6-phosphate isomerase; *K6PP* 6-phosphofructokinase; *ALDOA* aldolase A; *TPIS* triosephosphate isomerase; *GAPDH* glyceraldehydes 3-phosphate dehydrogenase; *PGK1* phosphoglycerate kinase 1; *KPYM* pyruvate kinase isozymes M1/M2; *ODPAT* pyruvate dehydrogenase E1 component subunit alpha; *ACLY* ATP-citrate synthase; and *IDHP* isocitrate dehydrogenase

and L7, and their citrate concentrations. The impact of elevated phosphorylation levels of T197 in isocitrate dehydrogenase in normal L2 and P2 samples was also unclear. We need a larger number of sample sets in order to validate these results and provide further insight into possible correlations between phosphorylated states of the enzymes and metabolomic profiles.

Levels of all the quantified TCA cycle intermediates were higher in tumor than normal prostate tissues (Fig. 3a), which may be related to the typically hypoxic microenvironment of prostate tissues, because most TCA cycle intermediates are known to increase under hypoxia, while their flux through the pathway remains low (Wiebe et al. 2008). Average prostate citrate concentrations were >11-fold higher than in lung. This was partly due to a high concentration of zinc in the prostate, which inhibits m-aconitase and results in citrate accumulation (Mycielska et al. 2009). Prostate tumor exhibits low zinc levels and elevated fatty acid synthesis consuming citrate, and thus its citrate level is typically lower than in normal tissues (Mycielska et al. 2009), which is, however, inconsistent with our results. Tumor citrate, *cis*-aconitate, and isocitrate levels in P1, P3 and P7 were consistently lower than their respective normal levels, leaving the possibility that zinc and m-aconitase activity levels may vary depending on a factor other than differentiation status.

Succinate, fumarate, and malate levels were markedly higher in both prostate and lung tumor tissues than their corresponding normal tissues (Fig. 3a), which was consistent with our previous results for colon and stomach tumor metabolomics (Hirayama et al. 2009). We recently obtained strong evidence that, especially under hypoxic and nutrient-deprived conditions, energy generation of cancer relies on fumarate respiration (Sakai et al. 2012; Tomitsuka et al. 2010). This confers upon cells the ability to produce ATP by harnessing fumarate to succinate conversion, rather than oxygen to water, as the final electron transport step via the reverse reaction of succinate dehydrogenase (Kita and Takamiya 2002). Accumulation of these metabolites in tumors may therefore be attributed to hyperactivity of fumarate respiration.

3.4 Tumor-specificity and organ-dependency in metabolic profiles

The metabolome data obtained from both lung and prostate tissues were collectively normalized and hierarchically clustered (Supplementary Fig. S4A). As a result, lung-versus-prostate differences in terms of the overall metabolomic profiles appeared to be more significant than normal-versus-tumor differences within the same organ, as observed in our previous comparative metabolome analyses in colon and stomach tissues (Hirayama et al. 2009). As expected, PCA with the collectively normalized data showed clear inter-organ differences along with the PC2 axis; however, the normal-versus-tumor distinctions were also observed along with the PC1 axis (Supplementary Fig. S4B). This suggests that, in the carcinogenic process, cells alter their metabolism with a certain 'metabolic directionality' that is independent of organ types while retaining much of the metabolism that is unique to their organs of origin. Metabolites that showed high correlations with the PC2 included several nucleosides, TCA cycle intermediates, and polyamines, which characterize the inter-organ metabolic differences (Supplementary Table S3). In contrast, most glucogenic amino acids such as Thr, Ile, Asn, Pro, His, Gln, and Ser were closely associated with the PC1 (Supplementary Table S3), suggesting that a hyper-production and/or -acquisition of a certain set of amino acids likely occurs in the course of tumorigenesis.

4 Conclusion

Overall tumor metabolomic profiles were found to be significantly different depending on tumor type in lung cancer and differentiation status in prostate cancer. Elevated tumor concentrations of almost all the amino acids, especially BCAAs, were identified in an organ-independent manner, and this trend was more prominent in SCC than the other tumor types in lung cancer and in poorly rather than moderately differentiated prostate cancer. Analyses with much more samples, however, are necessary in order to statistically confirm these unique subtype-specific metabolic fingerprint of cancer. In contrast, through our combined metabolomic and phosphorylated enzyme analyses, we found that glycolytic and TCA cycle intermediates,

levels of which are probably associated with enzyme phosphorylation levels, exhibited significant organ dependency, reaffirming that inter-organ metabolomic differences are generally more significant than normal-versus-tumor differences within the same organ. Nonetheless, metabolomic profiles of both lung and prostate tumors appear to have a common 'directionality' along with their increasing malignancy represented by high concentrations of a certain set of glucogenic amino acids. Taken together, we identified organ-dependent, tumor-specific, and tumor-pathology-dependent metabolic features, which highlights the need for a combined metabolomics and phosphoproteomics analysis on a broader scale with a larger number of sample sets for improving specificity and effectiveness of personalized anticancer therapeutics.

Acknowledgments The authors thank Dr. Masahiro Sugimoto for developing MasterHands software. This work was supported in part by a grant for the Third Term Comprehensive 10-year Strategy for Cancer Control from the Ministry of Health, Labour and Welfare (H.E.) and a grant from the Global COE Program entitled, "Human Metabolomic Systems Biology" (K.K.). This work was also supported by KAKENHI (Grant-in-Aid for Scientific Research) on Priority Areas "Systems Genomes" and on "Lifesurveyor" from the Ministry of Education, Culture, Sports, Science and Technology (MEXT) of Japan as well as research funds from the Yamagata prefectural government and the City of Tsuruoka (Y.O., M.T., and T.S.).

References

Baracos, V. E., & Mackenzie, M. L. (2006). Investigations of branched-chain amino acids and their metabolites in animal models of cancer. *Journal of Nutrition, 136*, 237S–242S.

Brand, I. A., & Soling, H. D. (1975). Activation and inactivation of rat liver phosphofructokinase by phosphorylation—dephosphorylation. *FEBS Letters, 57*, 163–168.

Fuchs, B. C., & Bode, B. P. (2005). Amino acid transporters ASCT2 and LAT1 in cancer: Partners in crime? *Seminars in Cancer Biology, 15*, 254–266.

Hall, M., Mickey, D. D., Wenger, A. S., & Silverman, L. M. (1985). Adenylate kinase: An oncodevelopmental marker in an animal model for human prostatic cancer. *Clinical Chemistry, 31*, 1689–1691.

Heiden, M. G. V., Cantley, L. C., & Thompson, C. B. (2009). Understanding the Warburg effect: The metabolic requirements of cell proliferation. *Science, 324*, 1029–1033.

Hirayama, A., Kami, K., Sugimoto, M., Sugawara, M., Toki, N., Onozuka, H., et al. (2009). Quantitative metabolome profiling of colon and stomach cancer microenvironment by capillary electrophoresis time-of-flight mass spectrometry. *Cancer Research, 69*, 4918–4925.

Ishihama, Y. (2005). Proteomic LC-MS systems using nanoscale liquid chromatography with tandem mass spectrometry. *Journal of Chromatography A, 1067*, 73–83.

Ishihama, Y., Rappsilber, J., Andersen, J. S., & Mann, M. (2002). Microcolumns with self-assembled particle frits for proteomics. *Journal of Chromatography A, 979*, 233–239.

Junker, B. H., Klukas, C., & Schreiber, F. (2006). VANTED: A system for advanced data analysis and visualization in the context of biological networks. *BMC Bioinformatics, 7*, 109.

Kita, K., & Takamiya, S. (2002). Electron-transfer complexes in *Ascaris* mitochondria. *Advances in Parasitology, 51*, 95–131.

Korotchkina, L. G., & Patel, M. S. (2001). Site specificity of four pyruvate dehydrogenase kinase isoenzymes toward the three phosphorylation sites of human pyruvate dehydrogenase. *Journal of Biological Chemistry, 276*, 37223–37229.

Kyono, Y., Sugiyama, N., Imami, K., Tomita, M., & Ishihama, Y. (2008). Successive and selective release of phosphorylated peptides captured by hydroxy acid-modified metal oxide chromatography. *Journal of Proteome Research, 7*, 4585–4593.

Le Mellay, V., Houben, R., Troppmair, J., Hagemann, C., Mazurek, S., Frey, U., et al. (2002). Regulation of glycolysis by Raf protein serine/threonine kinases. *Advances in Enzyme Regulation, 42*, 317–332.

Mycielska, M. E., Patel, A., Rizaner, N., Mazurek, M. P., Keun, H., Ganapathy, V., et al. (2009). Citrate transport and metabolism in mammalian cells: Prostate epithelial cells and prostate cancer. *BioEssays, 31*, 10–20.

Ohashi, Y., Hirayama, A., Ishikawa, T., Nakamura, S., Shimizu, K., Ueno, Y., et al. (2008). Depiction of metabolome changes in histidine-starved *Escherichia coli* by CE-TOFMS. *Molecular BioSystems, 4*, 135–147.

Olsen, J. V., de Godoy, L. M., Li, G., Macek, B., Mortensen, P., Pesch, R., et al. (2005). Parts per million mass accuracy on an Orbitrap mass spectrometer via lock mass injection into a C-trap. *Molecular and Cellular Proteomics, 4*, 2010–2021.

Patel, M. S., & Korotchkina, L. G. (2001). Regulation of mammalian pyruvate dehydrogenase complex by phosphorylation: Complexity of multiple phosphorylation sites and kinases. *Experimental & Molecular Medicine, 33*, 191–197.

Rappsilber, J., Ishihama, Y., & Mann, M. (2003). Stop and go extraction tips for matrix-assisted laser desorption/ionization, nanoelectrospray, and LC/MS sample pretreatment in proteomics. *Analytical Chemistry, 75*, 663–670.

Rappsilber, J., Mann, M., & Ishihama, Y. (2007). Protocol for micro-purification, enrichment, pre-fractionation and storage of peptides for proteomics using StageTips. *Nature Protocols, 2*, 1896–1906.

Saeed, A. I., Sharov, V., White, J., Li, J., Liang, W., Bhagabati, N., et al. (2003). TM4: A free, open-source system for microarray data management and analysis. *BioTechniques, 34*, 374–378.

Sakai, C., Tomitsuka, E., Esumi, H., Harada, S., & Kita, K. (2012). Mitochondrial fumarate reductase as a target of chemotherapy: From parasites to cancer cells. *Biochimica et Biophysica Acta, 1820*, 643–651.

Sugiyama, N., Masuda, T., Shinoda, K., Nakamura, A., Tomita, M., & Ishihama, Y. (2007). Phosphopeptide enrichment by aliphatic hydroxy acid-modified metal oxide chromatography for nano-LC-MS/MS in proteomics applications. *Molecular and Cellular Proteomics, 6*, 1103–1109.

Tomitsuka, E., Kita, K., & Esumi, H. (2010). The NADH-fumarate reductase system, a novel mitochondrial energy metabolism, is a new target for anticancer therapy in tumor microenvironments. *Annals of the New York Academy of Sciences, 1201*, 44–49.

Warburg, O. (1956). On the origin of cancer cells. *Science, 123*, 309–314.

Wiebe, M. G., Rintala, E., Tamminen, A., Simolin, H., Salusjarvi, L., Toivari, M., et al. (2008). Central carbon metabolism of *Saccharomyces cerevisiae* in anaerobic, oxygen-limited and fully aerobic steady-state conditions and following a shift to anaerobic conditions. *FEMS Yeast Research, 8*, 140–154.

European Journal of Medicinal Chemistry 60 (2013) 76–88

Contents lists available at SciVerse ScienceDirect

European Journal of Medicinal Chemistry

journal homepage: http://www.elsevier.com/locate/ejmech

Original article

Synthesis and antitumor evaluation of arctigenin derivatives based on antiausterity strategy

Naoki Kudou [a], Akira Taniguchi [b], Kenji Sugimoto [a], Yuji Matsuya [a], Masashi Kawasaki [c], Naoki Toyooka [b,d,*], Chika Miyoshi [e], Suresh Awale [f], Dya Fita Dibwe [g], Hiroyasu Esumi [e], Shigetoshi Kadota [g], Yasuhiro Tezuka [g,**]

[a] Graduate School of Medicine and Pharmaceutical Sciences, University of Toyama, 2630 Sugitani, Toyama, 930-0194, Japan
[b] Graduate School of Science and Technology for Research, University of Toyama, 3190 Gofuku, Toyama 930-8555, Japan
[c] Department of Liberal Arts and Sciences, Faculty of Engineering, Toyama Prefectural University, 5180 Kurokawa, Kosugi-Machi, Toyama 939-0398, Japan
[d] Graduate School of Innovative Life Science, University of Toyama, 3190 Gofuku, Toyama 930-8555, Japan
[e] Cancer Physiology Project, Research Center for Innovative Oncology, National Cancer Center Hospital East, Chiba, Japan
[f] Frontier Research Core for Life Sciences, University of Toyama, 2630 Sugitani, Toyama 930-0194, Japan
[g] Institute of Natural Medicine, University of Toyama, 2630 Sugitani, Toyama 930-0194, Japan

ARTICLE INFO

Article history:
Received 24 July 2012
Received in revised form
14 September 2012
Accepted 21 November 2012
Available online 28 November 2012

Keywords:
(−)-Arctigenin derivatives
Antiausteric activity
Synthesis
Pancreatic cancer

ABSTRACT

A series of new (−)-arctigenin derivatives with variably modified *O*-alkyl groups were synthesized and their preferential cytotoxicity was evaluated against human pancreatic cancer cell line PANC-1 under nutrient-deprived conditions. The results showed that monoethoxy derivative **4i** (PC_{50}, 0.49 μM), diethoxy derivative **4h** (PC_{50}, 0.66 μM), and triethoxy derivative **4m** (PC_{50}, 0.78 μM) showed the preferential cytotoxicities under nutrient-deprived conditions, which were identical to or more potent than (−)-arctigenin (**1**) (PC_{50}, 0.80 μM). Among them, we selected the triethoxy derivative **4m** and examined its *in vivo* antitumor activity using a mouse xenograft model. Triethoxy derivative **4m** exhibited also *in vivo* antitumor activity with the potency identical to or slightly more than (−)-arctigenin (**1**). These results would suggest that a modification of (−)-arctigenin structure could lead to a new drug based on the antiausterity strategy.

1. Introduction

Pancreatic cancer is the most aggressive cancer of all and has an exceptionally high global mortality rate, with an estimated 267,000 deaths worldwide in 2008. It ranks 8th or 9th as the most frequent cause of cancer death worldwide and is the 4th or 5th most frequent cause of cancer death in most developed countries, including the United States, Europe, and Japan [1]. Moreover, it has been estimated that the number of deaths from pancreatic cancer will reach 484,000 by 2030 [1]. Pancreatic cancer rapidly metastases and lead the patients to die in a short period of the diagnosis. Thus, the 5-year survival rate of the patients with the pancreatic cancer is the lowest among several cancers [2,3]. Though surgery is the only treatment method that offers any prospect of potential cure, chemotherapy with 5-fluorouracil and gemcitabine is also used for palliative therapy of advanced pancreatic cancer. However pancreatic cancer is largely resistant to most known chemotherapeutic agents including 5-fluorouracil and gemcitabine [4]. Therefore effective chemotherapeutic agents that target pancreatic cancer are urgently needed.

Tumor cells, in general, proliferate very fast, and the demand for essential nutrients, oxygen, *etc.* is always high. The immediate environment of cancers increasing in size, however, often becomes heterogeneous and some regions of large cancers often possess microenvironmental niches, which exhibit a significant gradient of critical metabolites including oxygen, glucose, other nutrients, and growth factors [5]. Thus, many cancer cells get the critical metabolites by randomly recruiting new blood vessels, a phenomenon commonly known as angiogenesis, to survive under such severe conditions. However, human pancreatic cancer survives with an extremely poor blood supply and becomes more malignant [6]. The method by which pancreatic cancer survives is by getting a remarkable tolerance to extreme nutrient starvation [7]. Therefore, it has been hypothesized that eliminating the tolerance of cancer cells to nutrition starvation

* Corresponding author. Graduate School of Science and Technology for Research, University of Toyama, 3190 Gofuku, Toyama 930-8555, Japan. Tel.: +81 76 445 6859.
** Corresponding author. Tel.: +81 76 434 7627; fax: +81 76 434 5059.
E-mail addresses: toyooka@eng.u-toyama.ac.jp (N. Toyooka), tezuka@inm.u-toyama.ac.jp (Y. Tezuka).

0223-5234/$ – see front matter © 2012 Elsevier Masson SAS. All rights reserved.
http://dx.doi.org/10.1016/j.ejmech.2012.11.031

may allow a novel biochemical approach known as "anti-austerity" for cancer therapy [8].

In this regard, we screened 500 medicinal plants used in Kampo medicine to identify agents that preferentially reduce the survival of nutrient-deprived human pancreatic cancer PANC-1 cells. The screen led to the isolation of (−)-arctigenin (**1**) as the active principle of *Arctium lappa* [9]. In addition to pancreatic cancer, arctigenin has been reported to inhibit lung, skin, and stomach cancers [10]. Thus, we started the synthetic work of arctigenin derivatives to obtain more effective drugs against pancreatic cancer. In *A. lappa*, (−)-arctigenin is mainly contained as its glucoside, arctiin, and after consumption arctiin was reported to be deglucosidated to (−)-arctigenin (**1**), followed by demethylation and dehydroxylation by intestinal bacteria to metabolites **I**–**V** [11]. As reported previously, (−)-arctigenin showed potent preferential cytotoxicity, whereas its glucoside, arctiin, showed no cytotoxicity [9]. In our preliminary examination, moreover, metabolites **I** and **V** (Fig. 1) showed weaker activity. These facts should suggest that the 4′-hydroxyl group should be important for the preferential cytotoxicity and that (−)-arctigenin is deactivated through the demethylation/demethoxylation. In addition, the enantiomer of (−)-arctigenin (**1**), (+)-arctigenin (Fig. 1), showed very weak preferential cytotoxicity, indicating the importance of the 2*R*,3*R* absolute stereochemistry of (−)-form. Thus, with an intention to improve the metabolism stability, we have synthesized 15 arctigenin derivatives **4a**–**o** with different alkoxy substituent and the 2*R*,3*R*-configuration, and the *in vitro* preferential cytotoxicity of them was characterized under nutrient-deprived conditions. Then, the triethoxy derivative **4m**, exhibiting the *in vitro* activity identical to **1** and having no methoxy group which may be metabolized, was selected and further evaluated the effect against tumor cell growth *in vivo* in a cancer xenograft mouse model.

2. Results and discussion

2.1. Chemistry

First we planned the synthesis of derivatives on the 3′ position of (−)-arctigenin. For this purpose, (−)-arctigenin (**1**) was converted to the diol **2** [12], which was transformed into 6 derivatives **4a**–**f** via selective protection of **2**, alkylation of **3**, followed by deprotection of the benzyl group (Scheme 1).

Next we planned the efficient and flexible synthesis of a variety of derivatives on the 3′, 3″, and 4″ positions of (−)-arctigenin.

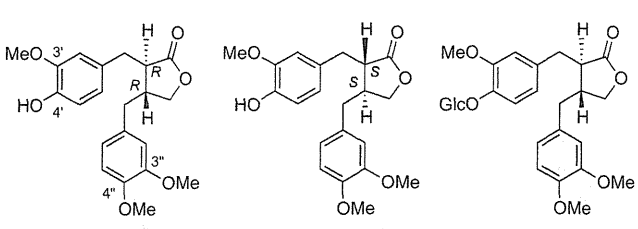

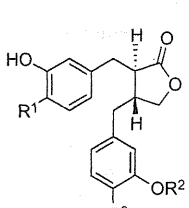

	R^1	R^2	R^3
I	OH	Me	OMe
II	H	Me	OMe
III	H	H	OMe
IV	H	H	OH
V	H	H	H

Fig. 1. Structures of (−)-arctigenin (**1**) and its analogs.

3,4-Dihydroxybenzaldehyde was converted to the alcohol **7** via known benzyl ether **5** [13] and aldehyde **6** [14]. Mono-alkylation of diethyl malonate with the mesylate of **7** afforded the ester **8**. Reduction of **8** and lipase-mediated transesterification of the resulting diol provided the mono-acetate (+)-**9**. The enantiomeric excess of (+)-**9** was determined to be 98% ee by the HPLC analysis using the chiral column (Chiralcel OJ). The absolute stereochemistry of (+)-**9** was determined by the comparison of the optical rotation with known lactone **13a**, prepared from (+)-**9** via mesylate **10**, benzyl ether **11**, and lactone **12a** as shown in Scheme 2. Other lactones **13b**–**f** were also prepared from (+)-**9**, and these lactones **13b**–**f** were alkylated on the α-position with several alkyl halides to afford the di-substituted lactones **14a**–**i**. Finally deprotection of the benzyl group furnished the desired derivatives **4g**–**o**.

From the comparison of the *in vitro* activity of the synthesized derivatives **4a**–**o** against the human pancreatic cancer cell line PANC-1, the triethoxy derivative **4m** was chosen as the potent candidate for the *in vivo* experiment. As the more effective synthesis of **4m**, we investigated the modified synthesis of the lactone **13d**. 3,4-Dihydroxybenzaldehyde was converted to the ester **17** via known aldehyde **15** [15] and alcohol **16** [16] as the same procedure for the synthesis of **8**. After reduction of **17**, lipase-mediated transesterification of the resulting diol afforded the mono-acetate **18**, whose enantiomeric excess was determined to be 98% ee again by the Mosher method. The mono-acetate **18** was then transformed into the lactone **13d** via mesylate **19** (Scheme 3).

2.2. In vitro preferential cytotoxicity of arctigenin derivatives

All of the (−)-arctigenin derivatives **4a**–**o** were evaluated for their *in vitro* preferential cytotoxic activity against human pancreatic cancer PANC-1 cells in nutrient-deprived medium (NDM). The PANC-1 cell line is highly resistant to nutrient starvation, and can survive in NDM even after 48 h of starvation [6,7,8]. However, this tolerance to nutrient starvation was remarkably eliminated by the tested compounds in a concentration-dependent manner. The tested compounds exhibited different potency of toxicity (Fig. 2) and their preferential cytotoxicities are obtained as the 50% cytotoxic concentration in NDM (PC_{50} value) (Table 1). Among the (−)-arctigenin derivatives **4a**–**o**, monoethoxy derivative **4i** showed the most potent preferential cytotoxicity (PC_{50}, 0.49 μM), followed by diethoxy derivative **4h** (PC_{50}, 0.66 μM) and triethoxy derivative **4m** (PC_{50}, 0.78 μM), which were identical to or more potent than (−)-arctigenin (**1**) (PC_{50}, 0.80 μM).

On the relationship between the substituents and the preferential activity, the 3′ position seems to favor smaller substituent since the PC_{50} values of **1** and **4a**–**d** increase in the order: **1** (MeO) < **4a** (EtO) = **4b** (*n*-PrO) < **4c** (*i*-PrO) < **4d** (*n*-BuO). This would suggest the importance of the 4′-hydroxy group for the preferential activity. On the other hand, there is not clear relationship on the substituents at the 3″ and 4″ positions, although smaller substituents seems to be favor.

The order of *in vitro* preferential cytotoxicity (PC_{50}) was **4i** > **4h** > **4m**. Whereas **4h** and **4i** have the methoxy groups which was reported to be demethylated and then deoxygenated by intestinal bacteria and/or hepatic enzyme [11]. Thus, we selected the triethoxy derivative **4m** to pursue a further examination, from a viewpoint of metabolism stability.

2.3. In vivo antitumor activity of triethoxy derivative *4m*

The triethoxy derivative **4m** showed the *in vitro* preferential cytotoxicity also against human pancreatic cancer cell line CAPAN-1 under glucose deficient conditions with a intensity similar to (−)-arctigenin (**1**) (Fig. 3). We used PANC-1 cell line for *in vitro*

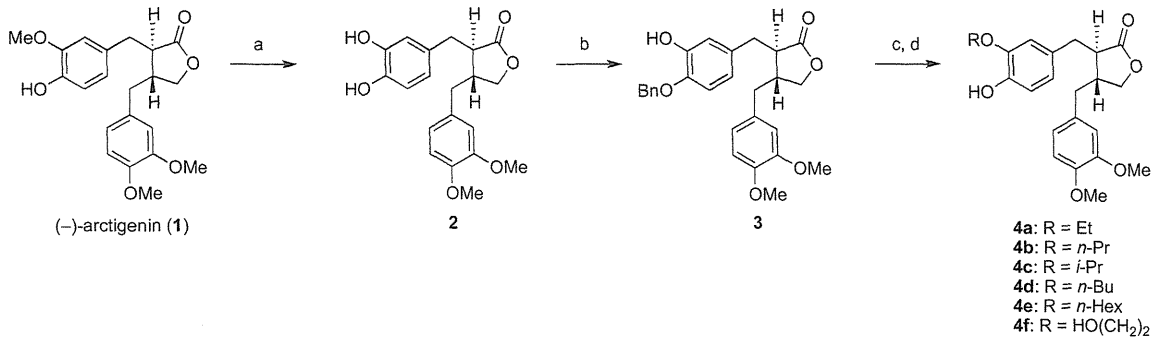

Scheme 1. Reagents and conditions: a: $AlCl_3$, pyridine, CH_2Cl_2, reflux (quant.); b: BnBr, K_2CO_3, KI, acetone, reflux (63%); c: RI or RBr, K_2CO_3, acetone, reflux for **4a–e** or 2-benzyloxyethanol, Ph_3P, DEAD, CH_2Cl_2, rt for **4f**; d: H_2, $Pd(OH)_2$, MeOH, rt.

study because of its ready growth [17], while mouse xenograft model can be prepared with CAPAN-1 cell line more easily than with PANC-1 cell line [18]. Thus, we used mouse xenograft model with CAPAN-1 cell line for comparing the *in vivo* effect of triethoxy derivative **4m** with (−)-arctigenin (**1**).

Mice were inoculated with 5×10^6 CAPAN-1 cells s.c. on the back and then administered triethoxy derivative **4m**, (−)-arctigenin (**1**), or vehicle, as described in Experimental. The body weight of the animals was monitored weekly (Fig. 4A) and no significant body weight loss was recognized in the treated group versus the vehicle control group at any time during the experimental period. This fact, together with the behavior of the treated animals, indicated that the tested compounds might have no toxicity at the dose used. The treatment was initiated from the 15th day by i.p. injection of the drug at the dose of 50 μg/mouse/d on 6 days of the week (or vehicle in the control group) until the 28th day. The tumor size was measured weekly. As is evident from the tumor growth curve shown in Fig. 4B, the tumor volume increased steadily in the control group, whereas the increase was significantly less prominent in the groups treated by triethoxy derivative **4m** or (−)-arctigenin (**1**). There was a significant difference in the tumor size at the day 21 between the groups treated by triethoxy derivative **4m** or (−)-arctigenin (**1**) and the control group ($P < 0.05$). Similarly, the mean wet weight and the size of the tumor were higher in the

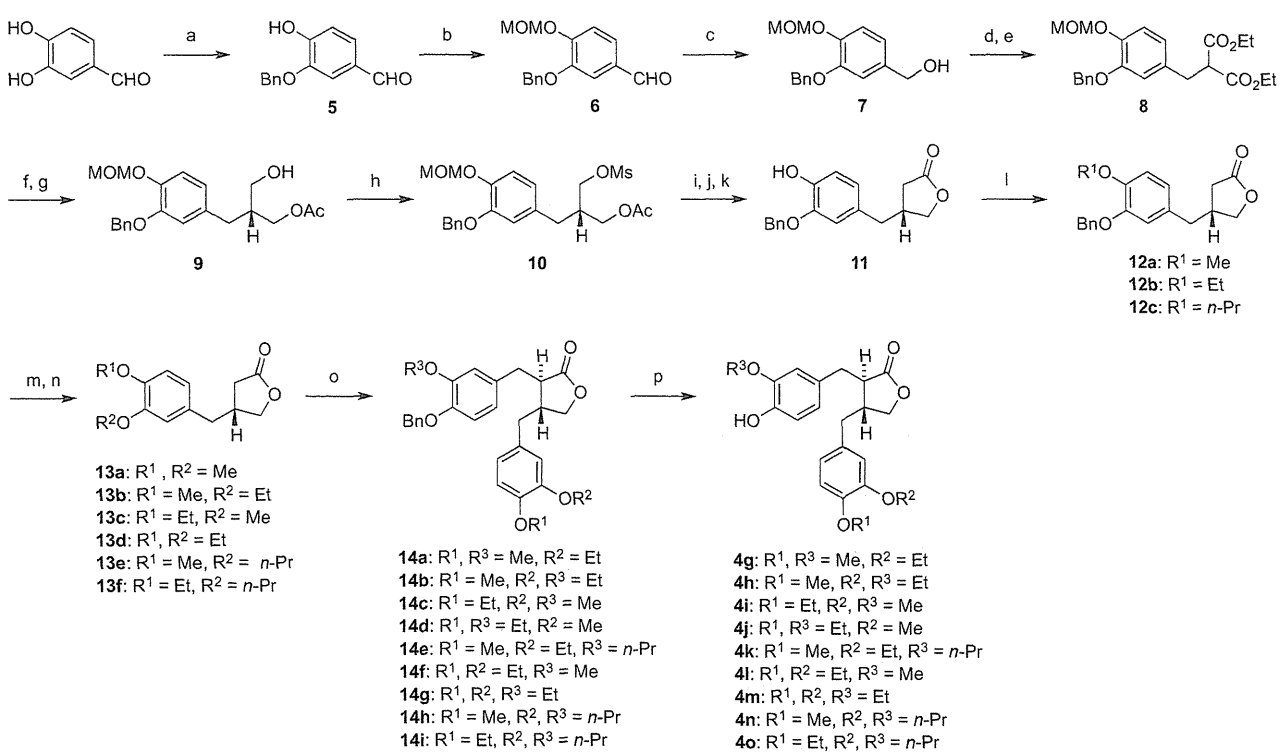

Scheme 2. Reagents and conditions: a: BnBr, K_2CO_3, KI, acetone, reflux (64%); b: MOMCl, DIPEA, CH_2Cl_2, rt (quant.); c: $NaBH_4$, MeOH, rt (95%); d: MsCl, Et_3N, CH_2Cl_2, rt; e: diethyl malonate NaH, DMF, rt (72% in 2 steps); f: $LiAlH_4$, THF, reflux; g: lipase-PS (Amano), vinyl acetate, *i*-Pr_2O–THF rt (80% in 2 steps, 98% ee); h: MsCl, Et_3N, CH_2Cl_2, rt; i: KCN, DMSO, 90 °C; j: LiOH, THF–H_2O, rt; k: 10% NaOH (aq), reflux, then 10% HCl (aq)–THF, rt (73% in 4 steps); l: MeI or EtI or *n*-PrBr, K_2CO_3, acetone, reflux (88% for **12a**, 86% for **12b**, 87% for **12c**); m: H_2, $Pd(OH)_2$, MeOH; *n*: MeI or EtI, K_2CO_3, acetone, reflux (55% in 2 steps for **13a**, 55% in 2 steps for **13b**, 55% in 2 steps for **13c**, 47% in 2 steps for **13d**, 80% in 2 steps for **13e**, 77% in 2 steps for **13f**); o: LiHMDS, substituted BnBr, HMPA, THF, −78 °C to rt (44% for **14a**, 59% for **14b**, 43% for **14c**, 53% for **14d**, 40% for **14e**; 48% for **14f**; 56% for **14g**, 49% for **14h**; 33% for **14i**); p: H_2, $Pd(OH)_2$, MeOH (89% for **4g**, 63% for **4h**, 57% for **4i**, 63% for **4j**, 56% for **4k**, 81% for **4l**, 66% for **4m**, 46% for **4n**, 63% for **4o**).

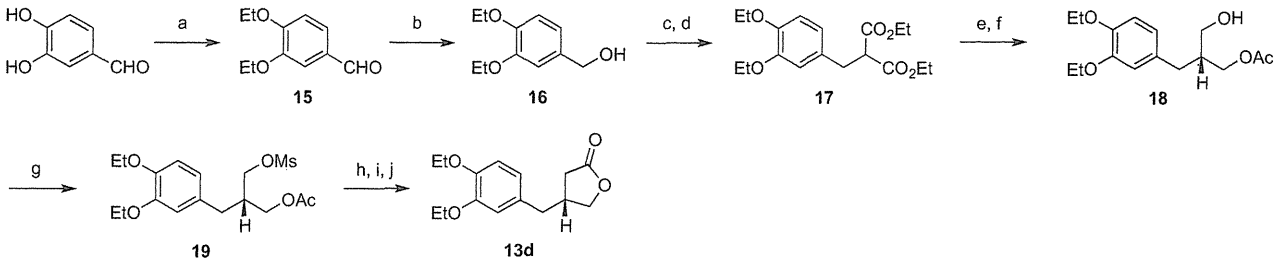

Scheme 3. Reagents and conditions: a: EtI, K_2CO_3, acetone, reflux (92%); b: $NaBH_4$, MeOH, rt (74%); c: MsCl, Et_3N, CH_2Cl_2, rt; d: diethyl malonate NaH, DMF, rt (87% in 2 steps); e: $LiAlH_4$, THF, reflux; f: lipase-PS (Amano), vinyl acetate, *i*-Pr_2O–THF rt (53% in 2 steps, 98% ee); g: MsCl, Et_3N, CH_2Cl_2, rt (79%); h: KCN, DMSO, 90 °C; i: LiOH, THF–H_2O, rt; j: 10% NaOH (aq), reflux, then 10% HCl (aq)-THF, rt (60% in 3 steps).

control group than the groups treated by triethoxy derivative **4m** or (−)-arctigenin (**1**) (Fig. 4C–F). These data indicate that triethoxy derivative **4m** also exerted antitumor activity *in vivo* with the potency identical to or slightly more than (−)-arctigenin (**1**).

3. Conclusion

In summary, a series of new (−)-arctigenin derivatives modified on *O*-alkyl groups were synthesized and their preferential cytotoxicity was evaluated against human pancreatic cancer cell line PANC-1 under nutrient-deprived conditions. The results showed that monoethoxy derivative **4i** (PC_{50}, 0.49 μM), diethoxy derivative **4h** (PC_{50}, 0.66 μM), and triethoxy derivative **4m** (PC_{50}, 0.78 μM) showed the preferential cytotoxicities under nutrient-deprived conditions, which were identical to or more potent than (−)-arctigenin (**1**) (PC_{50}, 0.80 μM). Among them, we selected the triethoxy derivative **4m** and examined *in vivo* antitumor activity with mouse xenograft model. Triethoxy derivative **4m** exhibited also *in vivo* antitumor activity with the potency identical to (−)-arctigenin (**1**). These results would suggest that a modification of (−)-arctigenin structure could lead to a new drug based on the antiausterity strategy.

4. Experimental

4.1. Chemistry

4.1.1. General conditions

Chemicals were purchased from Sigma–Aldrich, Merck, Nakalai Tesque, Wako Pure Chemicals, and Kanto Chemicals, and used without further purification. Column chromatography was done on Cica silica gel 60N (spherical, neutral; particle size, 40–50 μm, Kanto Chemical Co., Inc., Tokyo, Japan), while thin-layer chromatography (TLC) was performed on Merck silica gel $60F_{254}$ plates (Merck KGaA, Darmstadt, Germany). Melting points were taken on a Yanaco micromelting point apparatus and are uncorrected. The nuclear magnetic resonance (NMR) spectra were acquired in the specified solvent, in a Varian Gemini 300 spectrometer (300 and 75 MHz for ^1H and ^{13}C, respectively) or Varian UNITY plus 500 spectrometer (500 and 125 MHz for ^1H and ^{13}C, respectively) (Varian Inc., Palo Alto, CA, USA), with tetramethylsilane (TMS) as internal standard. The chemical shifts (δ) are reported in ppm downfield from TMS and coupling constants (J) are expressed in Hertz. Optical rotations were obtained in the specified solvent on a JASCO DIP-1000 digital polarimeter (JASCO Corp., Tokyo, Japan). IR spectra were measured with a JASCO FT/IR-460 Plus spectrophotometer (JASCO Corp.). The low-resolution mass spectra (MS) and high-resolution mass spectra (HRMS) were obtained with a Shimadzu GCMS-QP 500 mass spectrometer (Shimadzu Corp., Kyoto, Japan), JEOL D-200, or JEOL AX505 mass spectrometer (JEOL Ltd., Tokyo, Japan) in the electron impact mode at the ionization potential of 70 eV.

4.1.2. Synthesis of (−)-arctigenin derivatives ***4a–4f***

*4.1.2.1. (3R,4R)-3-(4-Benzyloxy-3-hydroxybenzyl)-4-(3,4-dimethoxybenzyl)dihydrofuran-2-one (**3**).* To a stirred solution of (3R,4R)-3-(3,4-dihydroxybenzyl)-4-(3,4-dimethoxybenzyl)dihydrofuran-2-one (**2**) [12] (65.4 mg, 0.18 mmol) in acetone (2 mL) were added K_2CO_3 (37.3 mg, 0.27 mmol), KI (5.97 mg, 0.036 mmol), and BnBr (21.4 μL, 0.18 mmol), and the resulting mixture was refluex for 5 h. After cooling, the reaction mixture was filtered, and the filtrate was evaporated. The residue was chromatographed on silica gel (10 g, hexane:acetone = 4:1) to give **3** (51.2 mg, 63%) as a pale yellow oil: ^1H NMR (300 MHz, $CDCl_3$) δ: 1.60 (1H, br), 2.47–2.63 (4H, m), 2.86–2.98 (2H, m), 3.80 (3H, s), 3.85 (3H, s), 3.80–3.89 (1H, m), 4.09–4.14 (1H, m), 5.13 (2H, s), 6.47–6.80 (6H, m), 7.28–7.44 (5H, m); ^{13}C NMR (75 MHz, $CDCl_3$) δ: 34.59, 38.19, 41.15, 46.53, 55.82, 55.98, 71.08, 71.21, 111.22, 111.72, 112.79, 113.95, 120.43, 121.20, 127.12, 127.69, 128.39, 130.30, 130.73, 136.98, 146.91, 147.67, 148.84, 149.63, 178.46; IR (neat): 1514 (C=C), 1769 (C=O) cm^{-1}; MS (EI) m/z 449 (M^+); HRMS (EI): calcd for $C_{27}H_{28}O_6$: 448.1886 (M^+), found: 448.2743; $[\alpha]_D^{26}$ −20.7 (*c* 0.85, $CHCl_3$).

*4.1.2.2. (3R,4R)-4-(3,4-Dimethoxybenzyl)-3-(3-ethoxy-4-hydroxybenzyl)dihydrofuran-2-one (**4a**).* To a stirred solution of **3** (44.7 mg, 0.10 mmol) in acetone (5 mL) were added K_2CO_3 (82.6 mg, 0.60 mmol), EtI (26.5 μL, 0.33 mmol), and the reaction mixture was refluxed for 48 h. After cooling, the reaction mixture was filtered, and the filtrate was evaporated. The residue was dissolved in MeOH (6 mL). To the solution was added 20% $Pd(OH)_2$ (10 mg), and the resulting suspension was stirred under a hydrogen atmosphere at 1 atm for 16 h. The catalyst was removed by filtration and the filtrate was evaporated. The residue was chromatographed on silica gel (7 g, hexane : acetone = 3:1) to give **4a** (13.4 mg, 35% in 2 steps) as a colorless oil: ^1H NMR (300 MHz, $CDCl_3$) δ: 1.41 (3H, t, J = 7.1 Hz), 2.42–2.64 (4H, m), 2.90 (2H, d, J = 5.2 Hz), 3.80 (3H, s), 3.84 (3H, s), 3.80–3.88 (1H, m), 4.02 (2H, q, J = 7.1 Hz), 4.08–4.13 (1H, m), 5.66 (1H, br), 6.46–6.75 (4H, m), 6.81 (1H, d, J = 8.0 Hz); ^{13}C NMR (75 MHz, $CDCl_3$) δ: 14.85, 30.94, 34.48, 38.15, 40.90, 46.58, 55.85, 64.38, 71.24, 111.11, 111.61, 112.29, 113.94, 120.43, 121.83, 129.20, 130.30, 144.47, 145.80, 147.62, 148.81, 178.51; IR (neat): 1516 (C=C), 1766 (C=O), 3446 (OH) cm^{-1}; MS (EI) m/z 386 (M^+); HRMS (EI): calcd for $C_{22}H_{26}O_6$: 386.1729 (M^+), found: 386.1724; $[\alpha]_D^{26}$ −20.5 (*c* 0.98, $CHCl_3$).

*4.1.2.3. (3R,4R)-4-(3,4-Dimethoxybenzyl)-3-(4-hydroxy-3-propoxybenzyl)dihydrofuran-2-one (**4b**).* By the procedure similar to synthesis of **4a**, (−)-arctigenin derivative **4b** was prepared from **3** and *n*-PrBr (18% in 2 steps) as a colorless oil: ^1H NMR (300 MHz, $CDCl_3$) δ: 1.04 (3H, t, J = 1.9 Hz), 1.77–1.87 (2H, m), 2.42–2.67 (4H, m), 2.81–3.01 (2H, m), 3.78–3.86 (7H, m), 3.90–4.00 (2H, m), 4.09–4.14 (1H, m), 5.59–5.63 (1H, br), 6.47–6.85 (6H, m); ^{13}C NMR (75 MHz, $CDCl_3$) δ: 10.60, 22.60, 29.34, 31.81, 34.55, 38.22, 41.49, 46.65, 53.80, 55.82, 70.35, 71.29, 111.71, 113.94, 115.27, 120.47, 121.85, 112.34, 129.28,

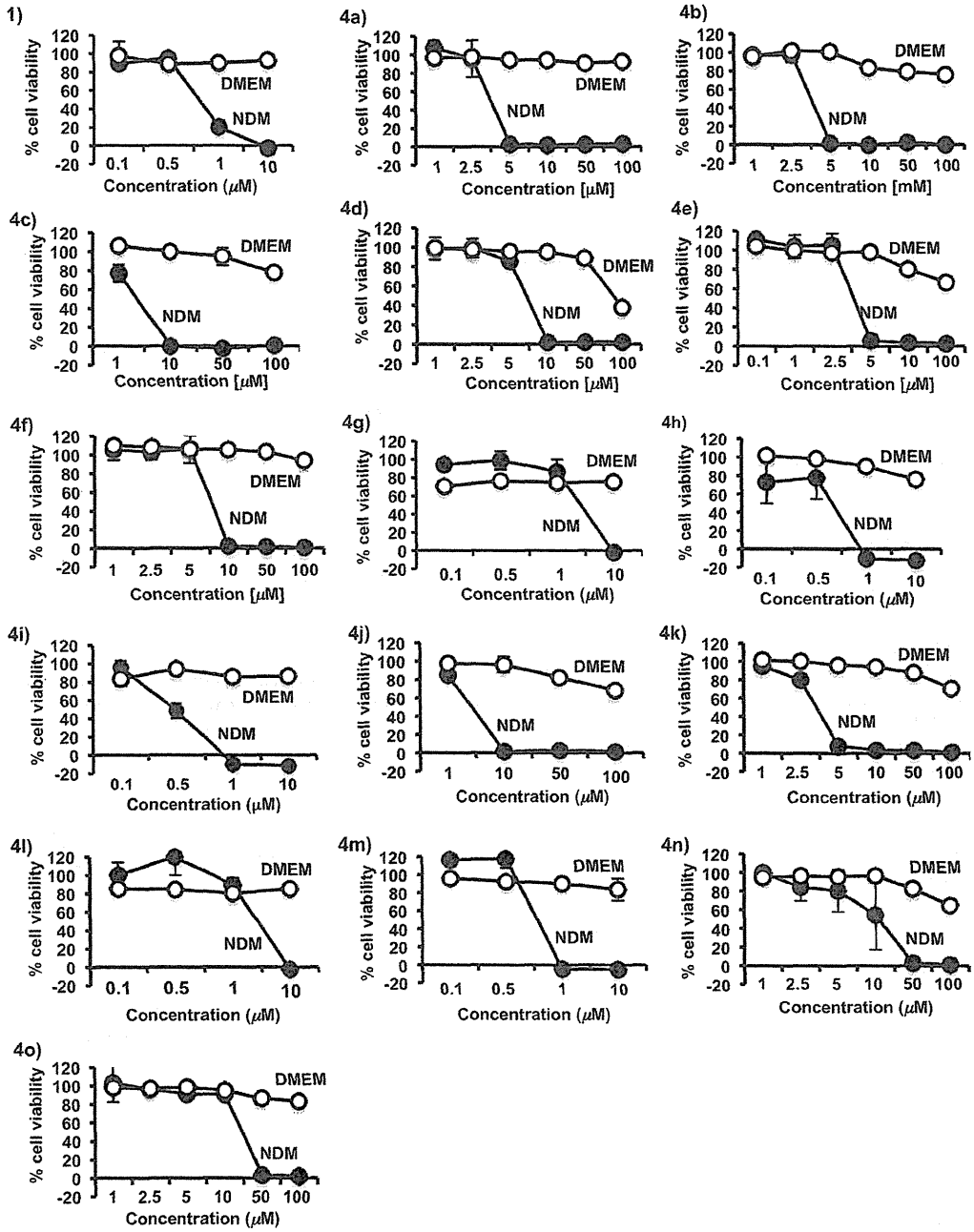

Fig. 2. Effects of (−)-arctigenin derivatives on cell survival in the PANC-1 cell line under nutrient-deprived conditions. Cells were seeded at a density of 2×10^4 per well in 96-well plates and incubated in fresh complete medium for 24 h. The cells were then washed with PBS and the medium was changed to nutrient-deprived medium (NDM, ●) or normal DMEM (○) together containing graded concentrations of (−)-arctigenin derivatives. Points, mean from triplicate experiments. The cell number at the start of the starvation was considered to be 100%. The cell count was measured by the WST-8 cell counting kit method, as described in experimental. The numbers **1** and **4a**–**o** mean the data of (−)-arctigenin (**1**) and (−)-arctigenin derivatives **4a**–**o**, respectively.

130.59, 144.52, 147.69, 178.54; IR (neat): 1456 (C=C), 1769 (C=O) cm^{-1}; MS (EI) *m/z* 400 (M^+); HRMS (EI): calcd for $C_{23}H_{28}O_6$: 400.1886 (M^+), found: 400.1893; $[\alpha]_D^{26}$ −15.7 (*c* 1.45, $CHCl_3$).

*4.1.2.4. (3R,4R)-4-(3,4-Dimethoxybenzyl)-3-(4-hydroxy-3-i-propoxybenzyl)dihydrofuran-2-one (**4c**).* By the procedure similar to synthesis of **4a**, (−)-arctigenin derivative **4c** was prepared from **3** and *i*-PrI (18% in 2 steps) as a pale yellow oil: ^1H NMR (300 MHz, $CDCl_3$) δ: 1.31–1.35 (6H, m), 1.59 (1H, br), 2.41–2.68 (4H, m), 2.80–3.00 (2H, m), 3.80–3.88 (7H, m), 4.07–4.12 (1H, m), 4.49–4.57 (1H, m), 6.48–6.84 (6H, m); ^{13}C NMR (75 MHz, $CDCl_3$) δ: 22.02, 34.39, 3.12, 41.45, 46.65, 55.81, 71.19, 111.25, 111.68, 113.41, 114.18, 115.49, 120.61, 122.09, 129.26, 130.43, 144.70, 145.48, 146.59, 147.84, 149.02, 178.72; IR (neat): 1716 (C=O), 3629 (OH) cm^{-1}; MS (EI) *m/z* 400 (M^+); HRMS (EI): calcd for $C_{23}H_{28}O_6$: 400.1886 (M^+), found: 400.1926; $[\alpha]_D^{24}$ −37.7 (*c* 0.41, $CHCl_3$).

*4.1.2.5. (3R,4R)-4-(3,4-Dimethoxybenzyl)-3-(4-hydroxy-3-butyloxybenzyl)dihydrofuran-2-one (**4d**).* By the procedure similar to synthesis of **4a**, (−)-arctigenin derivative **4d** was prepared from **3**

Table 1
Preferential cytotoxicity of (−)-arctigenin (**1**) and series of new (−)-arctigenin derivatives **4a–4o** against human pancreatic cancer PANC-1 cells in nutrient-deprived medium (NDM).

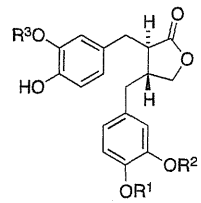

Compound	R^1	R^2	R^3	PC_{50} (μM)	Compound	R^1	R^2	R^3	PC_{50} (μM)
1 (arctigenin)	Me	Me	Me	0.80	**4h**	Me	Et	Et	0.66
4a	Me	Me	Et	3.74	**4i**	Et	Me	Me	0.49
4b	Me	Me	*n*-Pr	3.74	**4j**	Et	Me	Et	4.77
4c	Me	Me	*i*-Pr	4.16	**4k**	Me	Et	*n*-Pr	3.54
4d	Me	Me	*n*-Bu	7.14	**4l**	Et	Et	Me	4.85
4e	Me	Me	*n*-Hex	3.89	**4m**	Et	Et	Et	0.78
4f	Me	Me	$HO(CH_2)_2$	7.70	**4n**	Me	*n*-Pr	*n*-Pr	13.6
4g	Me	Et	Me	4.71	**4o**	Et	*n*-Pr	*n*-Pr	28.6

and *n*-BuBr (25% in 2 steps) as a colorless oil: ^{1}H NMR (300 MHz, $CDCl_3$) δ: 0.98 (3H, t, J = 7.1 Hz), 1.48 (2H, dd, J = 15.1, 7.1 Hz), 1.74–1.83 (2H, m), 2.41–2.66 (4H, m), 2.80–3.02 (2H, m), 3.82 (3H, s), 3.83 (3H, s), 3.85 (1H, m), 3.94–4.03 (2H, m), 4.08–4.14 (1H, m), 5.59 (1H, m), 6.50–6.84 (6H, m); ^{13}C NMR (75 MHz, $CDCl_3$) δ: 13.97, 19.32, 31.31, 55.82, 55.92, 68.60, 68.65, 71.21, 71.27, 111.19, 111.67, 112.32, 113.92, 120.46, 129.29, 130.34, 130.46, 144.52, 144.71, 145.59, 145.96, 147.69, 148.92, 178.53; IR (neat): 1515 (C=C), 1769 (C=O), 3446 (OH) cm^{-1}; MS (EI) m/z 414 (M^+); HRMS (EI): calcd for $C_{24}H_{30}O_6$: 414.2042 (M^+), found: 414.2000; $[\alpha]_D^{26}$ −20.2 (c 1.15, $CHCl_3$).

*4.1.2.6. (3R,4R)-4-(3,4-Dimethoxybenzyl)-3-(3-hexyloxy-4-hydroxybenzyl)dihydrofuran-2-one (**4e**).* By the procedure similar to synthesis of **4a**, (−)-arctigenin derivative **4e** was prepared from **3** and 1-bromohexane (35% in 2 steps) as a pale yellow oil: ^{1}H NMR (300 MHz, $CDCl_3$) δ: 0.90 (3H, t, J = 6.4 Hz), 1.25–1.27 (2H, m), 1.33–1.35 (4H, m), 1.45 (2H, m), 1.75–2.66 (4H, m), 2.81–3.01 (2H, m), 3.82 (3H, s), 3.85 (3H, s), 3.84–3.89 (1H, m), 3.94–4.02 (2H, m), 4.09–4.14 (1H, m), 5.56–5.61 (1H, m), 6.47–6.84 (6H, m); ^{13}C NMR (75 MHz, $CDCl_3$) δ: 14.11, 22.67, 25.78, 29.25, 31.62, 34.56, 38.22, 40.02, 46.65, 55.82, 68.92, 71.21, 111.19, 111.67, 112.32, 113.92, 115.25, 120.56, 121.83, 129.29, 130.43, 130.34, 144.52, 147.67, 148.92, 178.53; IR (neat): 1457 (C=C), 1764 (C=O), 3689 (OH) cm^{-1}; MS (EI) m/z 442 (M^+); HRMS (EI): calcd for $C_{26}H_{34}O_6$: 442.2355 (M^+), found: 442.2336; $[\alpha]_D^{26}$ −10.1 (c 0.65, $CHCl_3$).

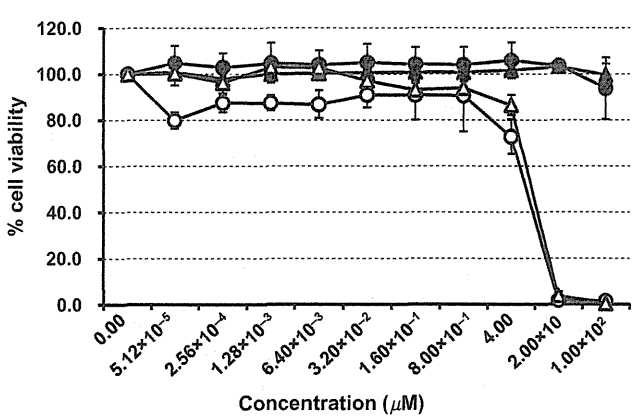

Fig. 3. Effect of triethoxy derivative **4m** and (−)-arctigenin (**1**) on cell survival in the CAPAN-1 cell line under glucose-deprived conditions. ●, (−)-arctigenin (**1**) in normal DMEM; ▲, triethoxy derivative **4m** in normal DMEM; ○, (−)-arctigenin (**1**) in glucose-deprived medium; △, triethoxy derivative **4m** in glucose-deprived medium.

*4.1.2.7. (3R,4R)-4-(3,4-Dimethoxybenzyl)-3-[4-hydroxy-3-(2-hydroxyethoxy)benzyl]dihydrofuran-2-one (**4f**).* By the procedure similar to synthesis of **4a**, (−)-arctigenin derivative **4f** was prepared from **3** and 2-benzyloxyethanol (20% in 2 steps) as a colorless oil: ^{1}H NMR (300 MHz, $CDCl_3$) δ: 2.42–2.59 (4H, m), 2.78–2.94 (2H, m), 3.76 (3H, s), 3.83 (3H, s), 3.73–3.80 (1H, m), 3.86–4.07 (6H, m), 4.13–4.16 (1H, m), 6.40–6.75 (4H, m), 6.81 (1H, d, J = 8.0 Hz); ^{13}C NMR (75 MHz, $CDCl_3$) δ: 28.24, 38.22, 40.69, 46.53, 55.72, 55.97, 61.08, 69.82, 71.45, 111.30, 111.56, 113.00, 115.02, 120.67, 122.55, 129.00, 130.44, 145.02, 146.10, 147.38, 148.72, 178.83; IR (neat): 1517 (C=C), 1765 (C=O), 3420 (OH) cm^{-1}; MS (EI) m/z 402 (M^+); HRMS (EI): calcd for $C_{23}H_{28}O_6$: 402.1679 (M^+), found: 402.1671; $[\alpha]_D^{26}$ −19.7 (c 1.10, $CHCl_3$).

*4.1.3. Synthesis of (−)-arctigenin derivatives **4g–4o***

*4.1.3.1. (4-Benzyloxy-3-methoxymethoxyphenyl)methanol (**7**).* To a stirred solution of 4-benzyloxy-3-methoxymethoxybenzaldehyde (**6**) [14] (7.03 g, 25.8 mmol) in MeOH (50 mL) was added $NaBH_4$ (3.88 g, 103 mmol) at 0 °C, and the resulting mixture was stirred at room temperature for 2 h. The reaction was quenched with H_2O (50 mL), and the aqueous mixture was extracted with CH_2Cl_2 (50 mL × 3). The organic extracts were combined, dried over $MgSO_4$. The solvent was removed under reduced pressure, and the residue was chromatographed on silica gel (40 g, hexane:acetone = 3:1) to give **7** (6.66 g, 95%) as a pale yellow oil: ^{1}H NMR (300 MHz, $CDCl_3$) δ: 1.26 (1H, br), 3.53 (3H, s), 5.01 (2H, s), 5.16 (2H, s), 5.24 (2H, s), 6.88–6.96 (2H, m), 7.16 (1H, d, J = 1.9 Hz), 7.30–7.45 (5H, m); ^{13}C NMR (75 MHz, $CDCl_3$) δ: 56.13, 64.64, 70.88, 95.40, 114.25, 116.22, 121.06, 126.98, 127.61, 128.27, 134.16, 136.82, 146.60, 148.19; IR (neat): 1511 (C=C), 3419 (OH) cm^{-1}; MS (EI) m/z 274 (M^+); HRMS (EI): calcd for $C_{16}H_{18}O_4$: 274.1205 (M^+), found: 274.1188.

*4.1.3.2. 2-(4-Benzyloxy-3-methoxymethoxybenzyl)malonic acid diethyl ester (**8**).* To a stirred solution of **7** (711 mg, 2.59 mmol) in CH_2Cl_2 (26 mL) were added NEt_3 (0.43 mL, 3.11 mmol) and MsCl (0.22 mL, 2.85 mmol) at 0 °C, and the reaction mixture was stirred at room temperature for 0.5 h. The reaction was quenched with sat. $NaHCO_3$ (aq) (20 mL), and the organic layer was separated. The aqueous layer was extracted with CH_2Cl_2 (30 mL × 3), and the organic layer and extracts were combined, dried over $MgSO_4$. The

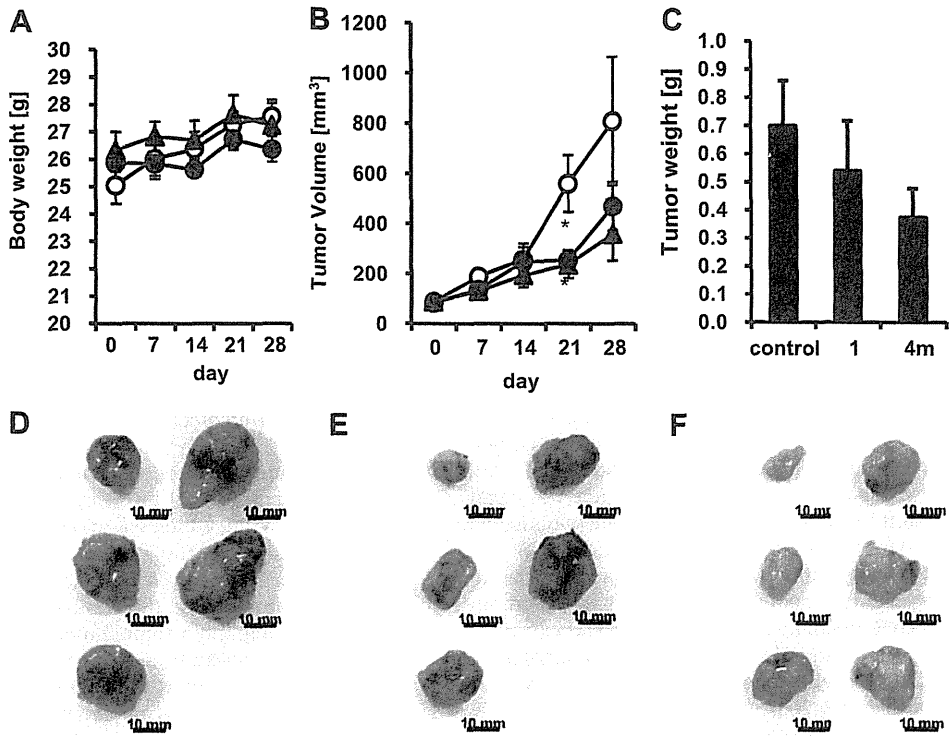

Fig. 4. Effect of triethoxy derivative **4m** and (−)-arctigenin (**1**) on the growth of CAPAN-1 cells in nude mice. A, body weight of mice. ○, control group ($n = 5$); ●, group treated with triethoxy derivative **4m** ($n = 6$); ▲, group treated with (−)-arctigenin (**1**) ($n = 5$). B, the tumor volume in the mice. ○, control group; ●, group treated with triethoxy derivative **4m**; ▲, group treated with (−)-arctigenin (**1**). C, wet weight of the tumor in the mice on the last day of the experiment. D–F, photographs of the tumor after sacrifice on the last day of control group, of group treated with (−)-arctigenin (**1**), and of group treated with triethoxy derivative **4m**, respectively.

solvent was removed under reduced pressure to give a pale yellow oil, which was used directly in the next step. To a stirred solution of diethyl malonate (0.79 mL, 5.18 mmol) in DMF (10 mL) was added NaH (60%, 207 mg, 5.18 mmol) at 0 °C, and the resulting mixture was stirred at room temperature for 1 h. To the solution was added a solution of the oil obtained above in DMF (2 mL) at 0 °C, and the reaction mixture was stirred at room temperature for 20 h. The reaction was quenched with sat. $NaHCO_3$ (aq) (10 mL), and the aqueous mixture was extracted with Et_2O (20 mL × 3). The organic extracts were combined, dried over $MgSO_4$, evaporated to give a pale yellow oil which was chromatographed on silica gel (20 g, hexane:acetone = 15:1) to give **8** (776 mg, 72% in 2 steps) as a pale yellow oil: ^{1}H NMR (300 MHz, $CDCl_3$) δ: 1.22 (6H, t, $J = 7.1$ Hz), 3.13 (2H, d, $J = 7.6$ Hz), 3.50 (3H, s), 3.60 (1H, t, $J = 7.6$ Hz), 4.16 (4H, q, $J = 7.1$ Hz), 5.11 (2H, s), 5.19 (2H, s), 6.74–6.83 (2H, m), 7.00 (1H, d, $J = 1.7$ Hz), 7.28–7.42 (5H, m); ^{13}C NMR (75 MHz, $CDCl_3$) δ: 14.05, 34.09, 53.93, 56.16, 61.35, 70.92, 95.64, 114.31, 117.98, 122.74, 127.01, 127.63, 128.31, 130.09, 136.95, 146.64, 147.71, 168.56; IR (neat): 1510 (C=C), 1732 (C=O) cm^{-1}; MS (EI) *m/z* 416 (M^+); HRMS (EI): calcd for $C_{23}H_{28}O_7$: 416.1835 (M^+), found: 416.1832.

*4.1.3.3. (R)-Acetic acid 3-(4-benzyloxy-3-methoxymethoxyphenyl)-2-hydroxymethylpropyl ester ((+)-**9**).* To a stirred solution of **8** (1.66 g, 3.98 mmol) in THF (40 mL) was added $LiAlH_4$ (378 mg, 9.96 mmol) at 0 °C, and the resulting suspension was refluxed for 12 h. The reaction was quenched with 10% NaOH (aq) (20 mL), and the mixture was extracted with AcOEt (20 mL × 5). The organic extracts were combined dried over $MgSO_4$, and the solvent was evaporated to give diol, which was used directly in the next step. To a stirred solution of the diol obtained above in *i*-Pr_2O–THF (20 mL, 4:1) were added lipase-PS (397 mg) and vinyl acetate (0.52 mL, 5.67 mmol), and the reaction mixture was stirred at room temperature for 2 h. The catalyst was filtered and the filtrate was evaporated to give residue, which was chromatographed on silica gel (30 g, hexane:acetone = 15:1) to give (+)-**9** (1.20 g, 80% in 2 steps) as a pale yellow oil. The enantiomeric excess of (+)-**9** was determined to be a 98% ee by the following HPLC analysis; chiralcel OJ (0.46 cm × 25 cm), hexane/2-propanol = 1/1, flow rate = 0.5 mL/min, $\lambda = 254$ nm, (+)-**9**; $t_R = 29.7$ min, (−)-**9**; 25.5 min ^{1}H NMR (300 MHz, $CDCl_3$) δ: 1.70 (1H, br), 2.09 (3H, s), 2.17 (1H, s), 2.55–2.62 (2H, m), 3.47–3.62 (2H, m), 3.52 (3H, s), 4.03–4.20 (2H, m), 5.13 (2H, s), 5.21 (2H, s), 6.72–6.98 (3H, m), 7.30–7.44 (5H, m); ^{13}C NMR (75 MHz, $CDCl_3$) δ: 20.99, 33.75, 42.47, 56.27, 62.08, 63.94, 71.14, 95.72, 114.534, 118.21, 122.92, 127.11, 127.71, 128.40, 132.46, 137.11, 146.82, 147.48, 171.47; IR (neat): 1739 (C=O), 3165 (OH) cm^{-1}; MS (EI) *m/z* 374 (M^+); HRMS (EI): calcd for $C_{21}H_{26}O_6$: 374.1729 (M^+), found: 374.1723; $[\alpha]_D^{26}$ +13.5 (*c* 1.14, $CHCl_3$).

*4.1.3.4. (R)-Acetic acid 3-(4-benzyloxy-3-methoxymethoxyphenyl)-2-methanesulfonyloxymethylpropyl ester (**10**).* To a stirred solution of (+)-**9** (666 mg, 1.78 mmol) in CH_2Cl_2 (8 mL) were added MsCl (0.15 mL, 1.95 mmol) and NEt_3 (0.32 mL, 2.31 mmol) at 0 °C, and the reaction mixture was stirred at room temperature for 0.5 h. The reaction was quenched with H_2O (8 mL), and the aqueous mixture was extracted with CH_2Cl_2 (10 mL × 3). The organic extracts were combined dried over $MgSO_4$, and evaporated. The residue was chromatographed on silica gel (30 g, hexane:acetone = 15:1) to give **10** (775 mg, 96%) as a pale yellow oil: ^{1}H NMR (300 MHz, $CDCl_3$) δ: 2.03 (3H, s), 2.27–2.34 (1H, m), 2.61 (2H, d, $J = 7.42$ Hz), 2.93 (3H, s), 3.47 (3H, s), 3.96–4.19 (4H, m), 5.08 (2H, s), 5.18 (2H, s), 6.69–6.95 (3H, m), 7.24–7.41 (5H, m); ^{13}C NMR (75 MHz, $CDCl_3$) δ: 20.91, 33.41, 37.26, 39.61, 56.29, 62.94, 68.34, 71.13, 95.67, 114.65, 118.05,

122.84, 127.12, 127.76, 128.42, 130.88, 136.98, 146.98, 147.72, 170.56; IR (KBr): 1242 (S=O), 1736 (C=O) cm^{-1}; MS (EI) *m/z* 452 (M^+); HRMS (EI): calcd for $C_{22}H_{28}O_8S$: 452.1505 (M^+), found: 452.1512; $[\alpha]_D^{25}$ +2.76 (*c* 1.40, $CHCl_3$).

*4.1.3.5. (R)-4-(4-Benzyloxy-3-hydeorxybenzyl)dihydrofuran-2-one (**11**).* To a stirred solution of **10** (993 mg, 2.19 mmol) in DMSO (20 mL) was added KCN (150 mg, 2.19 mmol), and the resulting mixture was heated at 90 °C for 3 h. After cooling, the reaction was quenched with H_2O (20 mL), and the aqueous mixture was extracted with Et_2O/AcOEt (1:1, 20 mL × 3). The organic extracts were combined, dried over $MgSO_4$, and evaporated to give cyanide, which was used directly in the next step. To a stirred solution of cyanide obtained above in THF–H_2O (3:1, 8 mL) was added LiOH·H_2O (91.9 mg, 2.19 mmol), and the reaction mixture was stirred at room temperature for 24 h. The reaction mixture was diluted with H_2O (10 mL), and the aqueous mixture was extracted with Et_2O (20 mL × 3). The organic extracts were combined, dried over $MgSO_4$, and evaporated to give alcohol, which was used directly in the next step. The alcohol obtained above was dissolved in 10% NaOH (aq) (10 mL), and the mixture was refluxed for 5 h. After cooling, 10% HCl (aq) (20 mL) and THF (20 mL) were added to the reaction mixture, and the resulting solution was stirred at room temperature for 50 h. The aqueous reaction mixture was extracted with Et_2O (30 mL × 3), and the organic extracts were combined, dried over $MgSO_4$, and evaporated to give a residue, which was chromatographed on silica gel (20 g, hexane:acetone = 3:1) to give **11** (479 mg, 73% in 4 steps) as a colorless solid: ^1H NMR (300 MHz, $CDCl_3$) δ: 2.17–2.32 (1H, m), 2.52–2.69 (3H, m), 2.74–2.86 (1H, m), 3.91–4.05 (1H, m), 4.30–4.36 (1H, m), 5.09 (2H, s), 5.67 (1H, br), 6.59–6.89 (3H, m), 7.36–7.85 (5H, m); ^{13}C NMR (75 MHz, $CDCl_3$) δ: 34.25, 37.22, 38.41, 71.22, 72.63, 112.26, 114.78, 120.04, 127.69, 128.32, 128.61, 131.72, 136.09, 144.50, 145.89, 176.68; IR (KBr): 1647 (C=O), 3445 (OH) cm^{-1}; MS (EI) *m/z* 298 (M^+); HRMS (EI): calcd for $C_{18}H_{18}O_4$: 298.1205 (M^+), found: 298.1204; $[\alpha]_D^{26}$ +5.6 (*c* 0.13, $CHCl_3$); mp: 137–139 °C.

*4.1.3.6. (R)-4-(4-Benzyloxy-3-methoxybenzyl)dihydrofuran-2-one (**12a**).* To a stirred solution of **11** (330 mg, 1.1 mmol) in acetone (15 mL) were added K_2CO_3 (168 mg, 1.2 mmol) and MeI (0.41 mL, 6.6 mmol), and the reaction mixture was refluxed for 24 h. After cooling, the insoluble materials were filtered, and the filtrate was evaporated to give a residue, which was chromatographed on silica gel (15 g, hexane:acetone = 4:1) to give **12a** (304 mg, 88%) as a colorless oil: ^1H NMR (300 MHz, $CDCl_3$) δ: 2.17 (2H, s), 2.24–2.30 (1H, m), 3.88 (3H, s), 4.03–4.05 (1H, m), 4.30–4.35 (1H, m), 5.13 (2H, s), 6.61–6.64 (2H, m), 6.81–6.83 (1H, m), 7.27–7.45 (5H, m); ^{13}C NMR (75 MHz, $CDCl_3$) δ: 34.29, 37.30, 38.64, 56.06, 71.11, 72.60, 112.32, 114.23, 120.52, 127.12, 127.72, 128.40, 131.25, 136.96, 146.91, 149.66, 176.65; IR (neat): 1654 (C=C), 1774 (C=O) cm^{-1}; MS (EI) *m/z* 312 (M^+); HRMS (EI): calcd for $C_{19}H_{20}O_4$: 312.1362 (M^+), found: 312.1380; $[\alpha]_D^{25}$ +4.9 (*c* 0.95, $CHCl_3$).

*4.1.3.7. (R)-4-(4-Benzyloxy-3-ethoxybenzyl)dihydrofuran-2-one (**12b**).* By the procedure similar to preparation of **12a**, **12b** was prepared from **11** and EtI (84%) as a pale yellow oil: ^1H NMR (300 MHz, $CDCl_3$) δ: 1.44 (3H, t, *J* = 4.4 Hz), 2.28 (1H, dd, *J* = 17.3, 6.9 Hz), 2.60 (1H, dd, *J* = 17.3, 8.0 Hz), 2.67–2.84 (3H, m), 4.02–4.13 (3H, m), 4.32 (1H, dd, *J* = 9.1, 6.9 Hz), 5.12 (2H, s), 6.60–6.69 (2H, m), 6.84 (1H, d, *J* = 8.2 Hz), 7.30–7.77 (5H, m); ^{13}C NMR (75 MHz, $CDCl_3$) δ: 15.03, 34.29, 37.31, 38.61, 64.74, 71.37, 72.62, 114.29, 115.22, 120.73, 127.08, 127.63, 128.34, 131.46, 137.20, 147.33, 149.18, 176.67; IR (neat): 1507 (C=C), 1772 cm^{-1} (C=O); MS (EI) *m/z* 326 (M^+); HRMS (EI): calcd for $C_{20}H_{22}O_4$: 326.1518 (M^+), found: 326.1523; $[\alpha]_D^{26}$ +3.4 (*c* 1.78, $CHCl_3$).

*4.1.3.8. (R)-4-(4-Benzyloxy-3-propoxybenzyl)dihydrofuran-2-one (**12c**).* By the procedure similar to preparation of **12a**, **12c** was prepared from **11** and *n*-PrBr (87%) as a colorless oil: ^1H NMR (600 MHz, $CDCl_3$) δ: 1.04 (3H, t, *J* = 7.0 Hz), 1.84 (2H, sextet, *J* = 7.0 Hz), 2.26 (1H, dd, *J* = 17.5, 7.0 Hz), 2.57 (1H, dd, *J* = 17.5, 8.1 Hz), 2.64–2.71 (2H, m), 2.74–2.83 (1H, m), 3.96 (2H, t, *J* = 7.0 Hz), 4.00 (1H, dd, *J* = 9.2, 5.9 Hz), 4.30 (1H, dd, *J* = 9.2, 7.0 Hz), 5.09 (2H, s), 6.60 (1H, d, *J* = 8.1 Hz), 6.67 (1H, s), 6.82 (1H, d, *J* = 8.1 Hz), 7.27–7.42 (5H, m); ^{13}C NMR (100 MHz, $CDCl_3$) δ: 10.46, 22.55, 34.07, 37.15, 38.43, 70.65, 71.32, 72.55, 114.28, 115.38, 120.69, 127.10, 127.63, 128.34, 131.61, 137.31, 147.37, 149.52, 176.84; IR (neat): 1508 (C=C), 1773 (C=O) cm^{-1}; MS (EI) *m/z* 340 (M^+); HRMS (EI): calcd for 340.1675 (M^+), found: 340.1667; $[\alpha]_D^{26}$ −1.0 (*c* 1.05, $CHCl_3$).

*4.1.3.9. (R)-4-(3,4-Dimethoxybenzyl)dihydrofuran-2-one (**13a**).* To a stirred solution of **12a** (302 mg, 0.97 mmol) in MeOH (5 mL) was added 20% $Pd(OH)_2$ (20 mg), and the resulting suspension was stirred under a hydrogen atmosphere at 1 atm for 15 h. The catalyst was removed by filtration and the filtrate was evaporated to give phenol, which was used directly in the next step. To a stirred solution of the phenol obtained above in acetone (10 mL) were added K_2CO_3 (201.1 mg, 1.46 mmol) and MeI (0.18 mL, 2.92 mmol), and the resulting mixture was refluxed for 19 h. After cooling, the insoluble materials were filtered, and the filtrate was evaporated to give a residue, which was chromatographed on silica gel (10 g, hexane:acetone = 4:1) to give **13a** (130 mg, 55% in 2 steps) as a pale yellow oil: ^1H NMR (300 MHz, $CDCl_3$) δ: 2.33 (1H, dd, *J* = 18.0, 9.3 Hz), 2.61 (1H, dd, *J* = 17.4, 8.1 Hz), 2.70–2.87 (3H, m), 3.87 (3H, s), 3.88 (3H, s), 4.05 (1H, dd, *J* = 9.3, 6.3 Hz), 4.33 (1H, dd, *J* = 9.3, 6.6 Hz), 6.66–6.72 (2H, m), 6.82 (1H, d, *J* = 8.1 Hz); $[\alpha]_D^{24}$ +22.2 (*c* 0.87, $CHCl_3$) (ref. [19], $[\alpha]_D^{25}$ +23.8).

*4.1.3.10. (R)-4-(4-Ethoxy-3-methoxybenzyl)dihydrofuran-2-one (**13b**).* By the procedure similar to preparation of **13a**, **13b** was prepared from **12a** and EtI (55% in 2 steps) as a pale yellow oil: ^1H NMR (300 MHz, $CDCl_3$) δ: 1.46 (3H, t, *J* = 7.1 Hz), 2.29 (1H, dd, *J* = 17.6, 6.9 Hz), 2.63 (1H, dd, *J* = 17.6, 8.0 Hz), 2.71–2.88 (3H, m), 3.86 (3H, s), 4.03 (1H, dd, *J* = 9.1, 6.9 Hz), 4.06 (2H, q, *J* = 7.1 Hz), 4.34 (1H, dd, *J* = 9.1, 6.9 Hz), 6.65–6.68 (2H, m), 6.81 (1H, d, *J* = 8.2 Hz); ^{13}C NMR (75 MHz, $CDCl_3$) δ: 14.92, 34.32, 37.36, 38.65, 55.98, 64.38, 72.63, 112.01, 112.84, 120.56, 130.59, 147.06, 149.26, 176.68; IR (neat): 1514 (C=C), 1778 (C=O) cm^{-1}; MS (EI) *m/z* 250 (M^+); HRMS (EI): calcd for $C_{14}H_{18}O_4$: 250.1205 (M^+), found: 250.1192; $[\alpha]_D^{24}$ +4.4 (*c* 1.66, $CHCl_3$).

*4.1.3.11. (R)-4-(3-Ethoxy-4-methoxybenzyl)dihydrofuran-2-one (**13c**).* By the procedure similar to preparation of **13a**, **13c** was prepared from **12b** and MeI (55% in 2 steps) as a pale yellow oil: ^1H NMR (300 MHz, $CDCl_3$) δ: 1.47 (3H, t, *J* = 6.9 Hz), 2.29 (1H, dd *J* = 17.3, 6.6 Hz), 2.61 (1H, dd, *J* = 17.3, 8.0 Hz), 2.67–2.87 (3H, m), 3.86(3H, s), 4.01–4.12 (3H, m), 4.34 (1H, dd, *J* = 9.1, 6.6 Hz), 6.62–6.69 (2H, m), 6.81 (1H, d, *J* = 8.0 Hz); ^{13}C NMR (75 MHz, $CDCl_3$) δ: 14.87, 34.24, 37.31, 38.54, 55.95, 64.35, 72.58, 111.61, 113.24, 120.54, 130.52, 148.01, 148.22, 176.63; IR (neat): 1541 (C=C), 1771 (C=O) cm^{-1}; MS (EI) *m/z* 250 (M^+); HRMS (EI): calcd for $C_{14}H_{18}O_4$: 250.1205 (M^+), found: 250.1207; $[\alpha]_D^{27}$ +4.4 (*c* 1.94, $CHCl_3$).

*4.1.3.12. (R)-4-(3,4-Diethoxybenzyl)dihydrofuran-2-one (**13d**).* By the procedure similar to preparation of **13a**, **13d** was prepared from **12b** and EtI (47% in 2 steps) as a pale yellow oil: ^1H NMR (300 MHz, $CDCl_3$) δ: 1.41–1.47 (6H, m), 2.28 (1H, dd, *J* = 17.3, 6.6 Hz), 2.59 (1H, dd, *J* = 17.3, 8.0 Hz), 2.67–2.86 (3H, m), 4.00–4.11 (5H, m), 4.32 (1H, dd, *J* = 9.3, 6.6 Hz), 6.64–6.67 (2H, m), 6.81 (1H, d, *J* = 8.5 Hz); ^{13}C NMR (75 MHz, $CDCl_3$) δ: 14.97, 34.30, 37.36, 38.61, 64.64, 64.69, 72.65,

113.70, 114.12, 120.78, 130.70, 147.53, 148.72, 176.68; IR (neat): 1507 (C=C), 1771 (C=O) cm^{-1}; MS (EI) *m/z* 264 (M^+); HRMS (EI): calcd for $C_{15}H_{20}O_4$: 264.1362 (M^+), found: 264.1369; $[\alpha]_D^{26}$ +5.4 (*c* 1.29, $CHCl_3$).

*4.1.3.13. (R)-4-(4-Methoxy-3-propoxybenzyl)dihydrofuran-2-one (**13e**).* By the procedure similar to preparation of **13a**, **13e** was prepared from **12c** and MeI (80% in 2 steps) as a pale yellow oil: ^1H NMR (400 MHz, $CDCl_3$) δ: 1.05 (3H, t, J = 7.1 Hz), 1.87 (2H, sextet, J = 7.1 Hz), 2.29 (1H, dd, J = 17.5, 6.8 Hz), 2.60 (1H, dd, J = 17.5, 8.1 Hz), 2.65–2.73 (2H, m), 2.77–2.84 (1H, m), 3.85 (1H, s), 3.96 (2H, t, J = 7.1 Hz), 4.03 (1H, dd, J = 9.3, 6.1 Hz), 4.33 (1H, dd, J = 9.3, 7.0 Hz), 6.67 (1H, s), 6.68 (1H, d, J = 7.8 Hz), 6.81 (1H, d, J = 7.8 Hz); ^{13}C NMR (100 MHz, $CDCl_3$) δ: 10.37, 22.44, 34.15, 37.23, 38.45, 56.00, 70.51, 72,57, 111.89, 113.52, 120.60, 130.67, 148.25, 148.62, 176.86; IR (neat): 1516 (C=C), 1778 (C=O) cm^{-1}; MS (EI) *m/z* 264 (M^+); HRMS(EI): calcd for $C_{15}H_{20}O_4$: 264.1362 (M^+), found: 264.1345; $[\alpha]_D^{26}$ +3.2 (*c* 1.05, $CHCl_3$).

*4.1.3.14. (R)-4-(4-Ethoxy-3-propoxybenzyl)dihydrofuran-2-one (**13f**).* By the procedure similar to preparation of **13a**, **13f** was prepared from **12c** and EtI (77% in 2 steps) as a pale yellow oil: ^1H NMR (400 MHz, $CDCl_3$) δ: 1.05 (3H, t, J = 7.0 Hz), 1,42 (3H, t, J = 6.8 Hz), 1.87 (2H, sextet, J = 7.0 Hz), 2.28 (1H, dd, J = 17.5, 7.0 Hz), 2.60 (1H, dd, J = 17.5, 8.0 Hz), 2.64–2.72 (2H, m), 2.74–2.85 (1H, m), 3.94 (2H, t, J = 7.0 Hz), 4.01–4.09 (3H, m), 4.32 (1H, dd, J = 9.1, 6.9 Hz), 6.64 (1H, s), 6.65 (1H, d, J = 8.0 Hz), 6.81 (1H, d, J = 8.0 Hz); ^{13}C NMR (100 MHz, $CDCl_3$) δ: 10.35, 14.79, 22.50, 34.10, 37.16, 38.38, 64.67, 70.72, 72.56, 114.05, 114.31, 120.78, 130.88, 147.64, 149.09, 176.85; IR (neat): 1510 (C=C), 1774 (C=O) cm^{-1}; MS (EI) *m/z* 278 (M^+); HRMS (EI): calcd for $C_{16}H_{22}O_4$: 278.1518 (M^+), found: 278.1512; $[\alpha]_D^{26}$ +1.2 (*c* 1.05, $CHCl_3$).

*4.1.3.15. (3R,4R)-3-(4-Benzyloxy-3-methoxybenzyl)-4-(3-ethoxy-4-methoxybenzyl)dihydrofuran-2-one (**14a**).* To a stirred solution of **13b** (29.6 mg, 0.12 mmol) in THF (2 mL) were added LiHMDS (1.6 M in THF, 0.12 mL, 0.18 mmol), HMPA (31 μL, 0.18 mmol) at −78 °C, and the resulting solution was stirred at the same temperature for 0.5 h. To the reaction mixture was added a solution of 4-benzyloxy-3-methoxybenzyl bromide [20] (52.3 mg, 0.19 mmol) in THF (2 mL), and allowed to warm to room temperature over 1 h, and then stirred at the same temperature for 20 h. The reaction was quenched with H_2O (4 mL), and the aqueous mixture was extracted with Et_2O (10 mL × 3). The organic extracts were combined, dried over $MgSO_4$, and evaporated to give residue, which was chromatographed on silica gel (10 g, hexane:acetone = 4:1) to give **14a** (25 mg, 44%) as a pale yellow oil: ^1H NMR (300 MHz, $CDCl_3$) δ: 1.44 (3H, t, J = 6.9 Hz), 2.46–2.65 (4H, m), 2.91–2.95 (2H, m), 3.79–3.90 (1H, m), 3.84 (6H, s), 4.01 (2H, q, J = 6.9 Hz), 4.08–4.20 (1H, m), 5.12 (2H, s), 6.50–6.80 (6H, m), 7.28–7.43 (5H, m); ^{13}C NMR (75 MHz, $CDCl_3$) δ: 14.77, 34.48, 38.02, 41.09, 46.42, 55.90, 64.28, 65.18, 71.03, 71.16, 111.57, 112.85, 113.35, 113.92, 114.02, 120.54, 121.28, 127.17, 127.20, 127.76, 128.46, 130.32, 130.82, 137.06, 147.01, 148.09, 148.26, 149.73, 178.65; IR (neat): 1515 (C=C), 1770 (C=O) cm^{-1}; MS (EI) *m/z* 476 (M^+); HRMS (EI): calcd for $C_{29}H_{32}O_6$: 476.2199 (M^+), found: 476.2197; $[\alpha]_D^{25}$ −16.4 (*c* 0.77, $CHCl_3$).

*4.1.3.16. (3R,4R)-3-(4-Benzyloxy-3-ethoxybenzyl)-4-(3-ethoxy-4-methoxybenzyl)dihydrofuran-2-one (**14b**).* By the procedure similar to preparation of **14a**, **14b** was prepared from **13b** and 4-benzyloxy-3-ethoxybenzyl bromide [21] (59%) as a pale yellow oil: ^1H NMR (300 MHz, $CDCl_3$) δ: 1.34–1.40 (6H, m), 2.36–2.51 (4H, m), 2.81–2.85 (2H, m), 3.71–3.78 (1H, m), 3.75 (3H, s), 3.90–4.05 (5H, m), 5.02 (2H, s), 6.40–6.80 (6H, m), 7.14–7.35 (5H, m); ^{13}C NMR (75 MHz, $CDCl_3$) δ: 14.75, 14.82, 34.43, 37.99, 41.05, 46.39, 55.86, 64.22, 64.47, 71.14, 71.26, 111.51, 113.24, 114.59, 114.97, 120.51, 121.39, 127.11, 127.64, 128.35, 130.31, 130.99, 137.27, 147.33, 148.03, 148.23, 149.24, 178.65; IR (neat): 1507 (C=C), 1771 (C=O) cm^{-1}; MS (EI) *m/z* 490 (M^+); HRMS (EI): calcd for $C_{30}H_{34}O_6$: 490.2355 (M^+), found: 490.2383; $[\alpha]_D^{26}$ −14.8 (*c* 1.46, $CHCl_3$).

*4.1.3.17. (3R,4R)-3-(4-Benzyloxy-3-methoxybenzyl)-4-(4-ethoxy-3-methoxybenzyl)dihydrofuran-2-one (**14c**).* By the procedure similar to preparation of **14a**, **14c** was prepared from **13c** and 4-benzyloxy-3-methoxybenzyl bromide [20] (43%) as a pale yellow oil: ^1H NMR (300 MHz, $CDCl_3$) δ: 1.45 (3H, t, J = 6.9 Hz), 2.47–2.63 (4H, m), 2.91–2.95 (2H, m), 3.84 (3H, s), 3.91 (3H, s), 3.91–3.95 (1H, m), 4.09 (2H, q, J = 6.9 Hz), 4.03–4.14 (1H, m), 5.16 (2H, s), 6.48–6.96 (6H, m), 7.28–7.45 (5H, m); ^{13}C NMR (75 MHz, $CDCl_3$) δ: 14.90, 34.58, 38.19, 41.13, 46.55, 55.98, 64.35, 65.29, 71.06, 110.88, 112.03, 112.82, 113.89, 113.97, 119.21, 120.44, 121.22, 127.69, 128.40, 130.26, 130.73, 134.03, 136.98, 146.91, 149.61, 178.49; IR (neat): 1261 (C=C), 1770 (C=O) cm^{-1}; MS (EI) *m/z* 476 (M^+); HRMS (EI): calcd for $C_{29}H_{32}O_6$: 476.2199 (M^+), found: 476.2209; $[\alpha]_D^{26}$ −9.0 (*c* 1.75, $CHCl_3$).

*4.1.3.18. (3R,4R)-3-(4-Benzyloxy-3-ethoxybenzyl)-4-(4-ethoxy-3-methoxybenzyl)dihydrofuran-2-one (**14d**).* By the procedure similar to preparation of **14a**, **14d** was prepared from **13c** and 4-benzyloxy-3-ethoxybenzyl bromide [21] (53%) as a pale yellow oil: ^1H NMR (300 MHz, $CDCl_3$) δ: 1.41–1.48 (6H, m), 2.44–2.67 (4H, m), 2.88–2.93 (2H, m), 3.79 (3H, s), 3.80–3.87 (1H, m), 4.02–4.14 (5H, m), 5.11 (2H, s), 6.45–6.96 (6H, m), 7.27–7.45 (5H, m); ^{13}C NMR (75 MHz, $CDCl_3$) δ: 14.62, 14.69, 30.69, 34.27 37.89, 40.87, 46.28, 55.66, 64.12, 64.35, 71.04, 71.12, 111.92, 112.61, 114.52, 114.84, 120.38, 121.31, 127.02, 127.52, 128.23, 130.29, 130.91, 137.17, 146.91, 147.20, 149.10, 178.55; IR (neat): 1515 (C=C), 1771 (C=O) cm^{-1}; MS (EI) *m/z* 490 (M^+); HRMS (EI): calcd for $C_{30}H_{34}O_6$: 490.2355 (M^+), found: 490.2383; $[\alpha]_D^{24}$ −17.9 (*c* 1.14, $CHCl_3$).

*4.1.3.19. (3R,4R)-3-(4-Benzyloxy-3-propoxybenzyl)-4-(3-ethoxy-4-methoxybenzyl)dihydrofuran-2-one (**14e**).* By the procedure similar to preparation of **14a**, **14e** was prepared from **13b** and 4-benzyloxy-3-propoxybenzyl bromide, prepared from 4-benzyl-3-propoxybenzaldehyde [22], (40%) as a pale yellow oil: ^1H NMR (400 MHz, $CDCl_3$) δ: 1.05 (3H, t, J = 7.1 Hz), 1.45 (3H, t, J = 7.8 Hz), 1.84 (2H, sextet, J = 7.1 Hz), 2.46–2.64 (4H, m), 2.86–2.99 (2H, m), 3.80–3.87 (4H, m), 3.94 (2H, t, J = 7.1 Hz), 4.00 (2H, q, J = 7.8 Hz), 4.06–4.11 (1H, m), 5.10 (2H, s), 6.48–6.82 (6H, m), 7.28–7.44 (5H, m); ^{13}C NMR (100 MHz, $CDCl_3$) δ: 10.47, 14.75, 22.56, 34.47, 38.00, 41.10, 46.40, 55.87, 64.25, 70.53, 71.35, 111.55, 113.29, 114.71, 115.25, 120.52, 121.37, 127.18, 127.57, 127.63, 128.33, 130.35, 131.126, 137.34, 147.40, 148.07, 148.26, 149.57, 178.64; IR (neat): 1514 (C=C), 1771 (C=O) cm^{-1}; MS (EI) *m/z* 504 (M^+); HRMS(EI): calcd for $C_{31}H_{36}O_6$: 504.2512 (M^+), found: 504.2538; $[\alpha]_D^{24}$ −10.7 (*c* 0.75, $CHCl_3$).

*4.1.3.20. (3R,4R)-3-(4-Benzyloxy-3-methoxybenzyl)-4-(3,4-diethoxybenzyl)dihydrofuran-2-one (**14f**).* By the procedure similar to preparation of **14a**, **14f** was prepared from **13d** and 4-benzyloxy-3-methoxybenzyl bromide [20] (48%) as a pale yellow oil: ^1H NMR (300 MHz, $CDCl_3$) δ: 1.41–1.59 (6H, m), 2.43–2.63 (4H, m), 2.91–2.95 (2H, m), 3.82–3.90 (1H, m), 3.85 (3H, s), 3.82–3.89 (1H, m), 3.97–4.12 (5H, m), 5.12 (2H, s), 6.49–6.80 (6H, m), 7.26–7.44 (5H, m); ^{13}C NMR (75 MHz, $CDCl_3$) δ: 14.85, 34.50, 38.07, 41.12, 46.50, 55.96, 64.59, 71.09, 71.21, 112.90, 113.63, 114.06, 114.20, 120.78, 121.33, 127.26, 127.81, 128.51, 130.50, 130.86, 137.12, 147.06, 147.60, 148.77, 149.76, 178.70; IR (neat): 1509 (C=C), 1772 (C=O) cm^{-1}; MS (EI) *m/z* 490 (M^+); HRMS (EI): calcd for $C_{30}H_{34}O_6$: 490.2355 (M^+), found: 490.2388; $[\alpha]_D^{25}$ −13.5 (*c* 0.98, $CHCl_3$).

*4.1.3.21. (3R,4R)-3-(4-Benzyloxy-3-ethoxybenzyl)-4-(3,4-diethoxybenzyl)dihydrofuran-2-one (**14g**).* By the procedure similar to preparation of **14a**, **14g** was prepared from **13d** and 4-benzyloxy-3-ethoxybenzyl bromide [21] (56%) as a pale yellow oil: ^1H NMR

(300 MHz, $CDCl_3$) δ: 1.41–1.44 (9H, m), 2.42–2.60 (4H, m), 3.82–3.86 (1H, m), 4.02–4.13 (7H, m), 5.11 (2H, s), 6.47–6.81 (6H, m), 7.27–7.44 (5H, m); ^{13}C NMR (75 MHz, $CDCl_3$) δ: 14.87, 34.50, 38.09, 41.11, 46.50, 64.60, 71.22, 71.37, 113.63, 114.17, 114.69, 115.08, 120.79, 121.48, 127.21, 127.71, 128.42, 130.53, 131.07, 137.35, 147.41, 147.95, 148.78, 149.32, 178.73; IR (neat): 1514 (C=C), 1770 (C=O) cm^{-1}; MS (EI) *m/z* 504 (M^+); HRMS (EI): calcd for $C_{31}H_{36}O_6$: 504.2512 (M^+), found: 504.6139; $[\alpha]_D^{25}$ −12.0 (*c* 0.58, $CHCl_3$).

*4.1.3.22. (3R,4R)-3-(4-Benzyloxy-3-propoxybenzyl)-4-(4-methoxy-3-propoxybenzyl)dihydrofuran-2-one (**14h**).* By the procedure similar to preparation of **14a**, **14h** was prepared from **13e** and 4-benzyloxy-3-propoxybenzyl bromide (49%) as a pale yellow oil: ^1H NMR (400 MHz, $CDCl_3$) δ: 1.02–1.08 (6H, m), 1.82–1.88 (4H, m), 2.45–2.63 (4H, m), 2.85–2.97 (2H, m), 3.83 (3H, s), 3.83–4.60 (6H, m), 5.10 (2H, s), 6.51–6.96 (6H, m), 7.28–7.45 (5H, m); ^{13}C NMR (100 MHz, $CDCl_3$) δ: 10.48, 14.84, 22.56, 34.46, 38.00, 41.07, 46.45, 64.71, 65.15, 70.55, 70.74, 71.18, 71.35, 71.37, 112.76, 114.42, 115.12, 119.34, 120.77, 121.40, 127.13, 127.15, 127.64, 128.34, 128.36, 130.63, 131.13, 137.36, 147.98, 149.58, 178.73; IR (neat): 1514 (C=C), 1771 (C=O) cm^{-1}; MS (EI) *m/z* 518 (M^+); HRMS(EI): calcd for $C_{32}H_{38}O_6$: 518.2668 (M^+), found: 518.2669; $[\alpha]_D^{25}$ −12.2 (*c* 0.75, $CHCl_3$).

*4.1.3.23. (3R,4R)-3-(4-Benzyloxy-3-propoxybenzyl)-4-(4-ethoxy-3-propoxybenzyl)dihydrofuran-2-one (**14i**).* By the procedure similar to preparation of **14a**, **14i** was prepared from **13f** and 4-benzyloxy-3-propoxybenzyl bromide (33%) as a pale yellow oil: ^1H NMR (400 MHz, $CDCl_3$) δ: 1.02–1.08 (6H, m), 1.41 (3H, t, *J* = 7.1 Hz), 1.80–1.91 (4H, m), 2.41–2.63 (4H, m), 2.87–2.94 (2H, m), 3.82–3.96 (5H, m), 4.01 (2H, q, *J* = 7.1 Hz), 4.05–4.10 (1H, m), 5.10 (2H, s), 6.49–6.96 (6H, m), 7.28–7.45 (5H, m); ^{13}C NMR (100 MHz, $CDCl_3$) δ: 10.50, 22.59, 34.51, 38.05, 41.12, 46.48, 56.00, 65.22, 70.57, 71.40, 111.86, 112.79, 113.63, 114.72, 115.30, 119.36, 120.55, 121.40, 127.16, 127.28, 127.65, 128.36, 130.41, 131.16, 137.37, 147.43, 148.25, 148.58, 149.62, 178.70; IR (neat): 1508 (C=C), 1767 (C=O) cm^{-1}; MS (EI) *m/z* 532 (M^+); HRMS (EI): calcd for $C_{33}H_{40}O_6$: 532.2825 (M^+), found: 518.2817; $[\alpha]_D^{25}$ −6.3 (*c* 0.80, $CHCl_3$).

*4.1.3.24. (3R,4R)-4-(3-Ethoxy-4-methoxybenzyl)-3-(4-hydroxy-3-methoxybenzyl)dihydrofuran-2-one (**4g**).* To a stirred solution of **14a** (47.5 mg, 0.10 mmol) in MeOH (5 mL) was added 20% $Pd(OH)_2$ (20 mg), and the resulting suspension was stirred under a hydrogen atmosphere at 1 atm for 20 h. The catalyst was removed by filtration and the filtrate was evaporated to give a residue, which was chromatographed on silica gel (10 g, hexane:acetone = 3:1) to give **4g** (34.1 mg, 89%) as a pale yellow oil: ^1H NMR (300 MHz, $CDCl_3$) δ: 1.45 (3H, t, *J* = 7.1 Hz), 2.43–2.65 (4H, m), 2.91–2.94 (2H, m), 3.81–3.89 (1H, m), 3.83 (3H, s), 3.84 (3H, s), 4.01 (2H, q, *J* = 7.1 Hz), 4.12 (1H, dd, *J* = 9.1, 6.9 Hz), 5.53 (1H, s), 6.47–6.65 (4H, m), 6.69 (1H, d, *J* = 8.0 Hz), 6.82 (1H, d, *J* = 8.0 Hz); ^{13}C NMR (75 MHz, $CDCl_3$) δ: 14.80, 30.91, 34.46, 38.09, 40.95, 46.55, 55.83, 55.94, 64.30, 71.27, 99.88, 111.54, 113.26, 114.10, 120.58, 122.08, 129.47, 130.35, 144.52, 146.67, 148.11, 148.33; IR (neat): 1513 (C=C), 1771 (C=O) cm^{-1}; MS (EI) *m/z* 386 (M^+); HRMS (EI): calcd for $C_{22}H_{26}O_6$: 386.1729 (M^+), found: 386.1693; $[\alpha]_D^{25}$ −17.2 (*c* 1.44, $CHCl_3$).

*4.1.3.25. (3R,4R)-4-(3-Ethoxy-4-hydroxybenzyl)-3-(3-ethoxy-4-methoxybenzyl)dihydrofuran-2-one (**4h**).* By the procedure similar to preparation of **4g**, **4h** was prepared from **14b** (63%) as a pale yellow oil: ^1H NMR (300 MHz, $CDCl_3$) δ: 1.42–1.47 (6H, m), 2.46–2.63 (4H, m), 2.92 (2H, d, *J* = 5.8 Hz), 3.81–3.89 (1H, m), 3.84 (3H, s), 3.97–4.12 (5H, m), 5.60 (1H, br), 6.48–6.84 (6H, m); ^{13}C NMR (75 MHz, $CDCl_3$) δ: 14.78, 30.88, 34.39, 38.04, 40.90, 46.53, 55.90, 64.26, 64.39, 71.24, 111.51, 112.37, 113.21, 114.01, 120.55, 121.95, 129.34, 130.35, 144.59, 145.93, 148.08, 148.03, 178.74; IR (neat): 1516 (C=C), 1768 (C=O) cm^{-1}; MS (EI) *m/z* 400 (M^+); HRMS (EI): calcd for $C_{23}H_{28}O_6$: 400.1886 (M^+), found: 400.1868; $[\alpha]_D^{27}$ −16.9 (*c* 1.13, $CHCl_3$).

*4.1.3.26. (3R,4R)-4-(4-Ethoxy-3-methoxybenzyl)-3-(4-hydroxy-3-methoxybenzyl)dihydrofuran-2-one (**4i**).* By the procedure similar to preparation of **4g**, **4i** was prepared from **14c** (57%) as a pale yellow oil: ^1H NMR (300 MHz, $CDCl_3$) δ: 1.45 (3H, t, *J* = 7.1 Hz), 2.44–2.67 (4H, m), 2.93 (2H, d, *J* = 5.8 Hz), 3.81 (3H, s), 3.82 (3H, s), 3.84–3.99 (1H, m), 4.03–4.15 (1H, m), 4.08 (2H, q, *J* = 7.1 Hz), 5.30 (1H, br), 6.47–6.66 (4H, m), 6.75 (1H, d, *J* = 8.0 Hz), 6.82 (1H, d, *J* = 8.0 Hz); ^{13}C NMR (75 MHz, $CDCl_3$) δ: 14.90, 30.99, 34.53, 38.22, 40.97, 46.63, 55.89, 64.35, 71.31, 111.48, 112.00, 112.71, 114.04, 120.47, 122.01, 129.37, 130.30, 144.39, 146.54, 146.99, 149.18, 178.56; IR (neat): 1749 (C=O), 3648 (OH) cm^{-1}; MS (EI) *m/z* 386 (M^+); HRMS (EI): calcd for $C_{22}H_{26}O_6$: 386.1729 (M^+), found: 386.1693; $[\alpha]_D^{26}$ −9.5 (*c* 0.71, $CHCl_3$).

*4.1.3.27. (3R,4R)-4-(3-Ethoxy-4-hydroxybenzyl)-3-(4-ethoxy-3-methoxybenzyl)dihydrofuran-2-one (**4j**).* By the procedure similar to preparation of **4g**, **4j** was prepared from **14d** (63%) as a pale yellow oil: ^1H NMR (300 MHz, $CDCl_3$) δ: 1.39–1.46 (6H, m), 2.41–2.66 (4H, m), 2.91 (2H, d, *J* = 6.0 Hz), 3.80 (3H, s), 3.81–3.87 (1H, m), 4.00–4.10 (5H, m), 5.64 (1H, br), 6.47–6.65 (4H, m), 6.74 (1H, d, *J* = 8.2 Hz), 6.82 (1H, d, *J* = 8.2 Hz); ^{13}C NMR (75 MHz, $CDCl_3$) δ: 14.75, 30.86, 34.35, 38.06, 40.84, 46.54, 55.78, 64.26, 64.37, 71.24, 111.98, 112.38, 112.69, 114.00, 120.52, 121.95, 129.32, 130.38, 144.58, 145.91, 147.07, 149.25; IR (neat): 1771 (C=O), 3548 (OH) cm^{-1}; MS (EI) *m/z* 400 (M^+); HRMS (EI): calcd for $C_{23}H_{28}O_6$: 400.1886 (M^+), found: 400.1897; $[\alpha]_D^{26}$ −12.4 (*c* 1.04, $CHCl_3$).

*4.1.3.28. (3R,4R)-4-(3-Ethoxy-4-methoxybenzyl)-3-(4-hydroxy-3-propoxybenzyl)dihydrofuran-2-one (**4k**).* By the procedure similar to preparation of **4g**, **4k** was prepared from **14e** (56%) as a pale yellow oil: ^1H NMR (400 MHz, $CDCl_3$) δ: 1.04 (3H, t, *J* = 7.4 Hz), 1.45 (3H, t, *J* = 7.1 Hz), 1.82 (2H, sextet, *J* = 7.4 Hz), 2.48–2.63 (4H, m), 2.91 (2H, d, *J* = 5.9 Hz), 3.81–3.88 (4H, m), 3.93 (2H, t, *J* = 7.4 Hz), 4.02 (2H, q, *J* = 7.1 Hz), 4.06–4.12 (1H, m), 5.57 (1H, s), 6.48 (1H, s), 6.54 (1H, d, *J* = 10.2 Hz), 6.60 (1H, d, *J* = 10.2 Hz), 6.66 (1H,s), 6.75 (1H, d, *J* = 8.2 Hz), 6.82 (1H, d, *J* = 8.2 Hz); ^{13}C NMR (100 MHz, $CDCl_3$) δ: 10.43, 14.79, 22.49, 34.41, 38.05, 40.95, 46.54, 55.92, 64.29, 70.32, 71.24, 111.55, 112.43, 113.26, 114.01, 120.57, 121.93, 129.37, 130.37, 144.64, 146.05, 148.12, 148.33, 178.75; IR (neat): 1516 (C=C), 1769 (C=O), 3589 (OH) cm^{-1}; MS (EI) *m/z* 414 (M^+); HRMS (EI): calcd for $C_{24}H_{30}O_6$: 414.2042 (M^+), found: 414.2046; $[\alpha]_D^{26}$ −10.6 (*c* 1.10, $CHCl_3$).

*4.1.3.29. (3R,4R)-4-(3,4-Diethoxybenzyl)-3-(4-hydroxy-3-methoxybenzyl)dihydrofuran-2-one (**4l**).* By the procedure similar to preparation of **4g**, **4l** was prepared from **14f** (81%) as a pale yellow oil: ^1H NMR (300 MHz, $CDCl_3$) δ: 1.25–1.45 (6H, m), 2.44–2.66 (4H, m), 2.92 (2H, d, *J* = 6.0 Hz), 3.83 (3H, s), 3.85–3.89 (1H, m), 3.98–4.13 (5H, m), 5.55 (1H, br), 6.49–6.67 (4H, m), 6.76 (1H, d, *J* = 7.8 Hz), 6.82 (1H, d, *J* = 7.8 Hz); ^{13}C NMR (75 MHz, $CDCl_3$) δ: 14.84, 30.91, 34.40, 38.04, 40.94, 46.56, 55.84, 64.58, 71.25, 111.56, 113.60, 114.11, 120.77, 122.10, 129.47, 130.51, 144.51, 146.65, 147.57, 148.78, 178.75; IR (neat): 1766 (C=O), 2978 (OH) cm^{-1}; MS (EI) *m/z* 400 (M^+); HRMS (EI): calcd for $C_{23}H_{28}O_6$: 400.1886 (M^+), found: 400.1858; $[\alpha]_D^{27}$ −16.0 (*c* 1.33, $CHCl_3$).

*4.1.3.30. (3R,4R)-4-(3,4-Diethoxybenzyl)-3-(4-hydroxy-3-ethoxybenzyl)dihydrofuran-2-one (**4m**).* By the procedure similar to preparation of **4g**, **4m** was prepared from **14g** (66%) as a pale yellow oil: ^1H NMR (300 MHz, $CDCl_3$) δ: 1.40–1.46 (9H, m), 2.42–2.67 (4H, m), 2.91 (2H, d, *J* = 5.7 Hz), 3.85 (1H, dd, *J* = 9.1, 7.4 Hz), 3.97–4.12

(7H, m), 5.59 (1H, br), 6.49–6.66 (4H, m), 6.75 (1H, d, J = 8.0 Hz), 6.82 (1H, d, J = 8.0 Hz); ^{13}C NMR (75 MHz, $CDCl_3$) δ: 14.81, 14.85, 34.39, 38.06, 40.92, 46.58, 64.42, 64.59, 71.27, 112.43, 113.62, 114.05, 114.10, 120.80, 122.00, 129.37, 130.53, 144.61, 145.94, 147.58, 148.80, 178.79; IR (neat): 1516 (C=C), 1761 (C=O) cm^{-1}; MS (EI) m/z 414 (M^+); HRMS (EI): calcd for $C_{24}H_{30}O_6$: 414.2042 (M^+), found: 414.2024; $[\alpha]_D^{25}$ −14.0 (c 0.70, $CHCl_3$).

*4.1.3.31. (3R,4R)-4-(4-Methoxy-3-propoxybenzyl)-3-(4-hydroxy-3-propoxybenzyl)dihydrofuran-2-one (**4n**).* By the procedure similar to preparation of **4g**, **4n** was prepared from **14h** (46%) as a pale yellow oil: ^{1}H NMR (400 MHz, $CDCl_3$) δ: 1.02–1.07 (6H, m), 1.78–1.90 (4H, m), 2.47–2.65 (4H, m), 2.92 (2H, d, J = 5.9 Hz), 3.81 (3H, s), 3.81–3.95 (5H, m), 4.08–4.12 (1H, m), 5.56 (1H, br), 6.50 (1H, s), 6.53 (1H, d, J = 7.9 Hz), 6.60 (1H, d, J = 7.9 Hz), 6.66 (1H, s), 6.75 (1H, d, J = 8.2 Hz), 6.82 (1H, d, J = 8.2 Hz); ^{13}C NMR (100 MHz, $CDCl_3$) δ:10.39, 22.45, 22.47, 34.37, 38.01, 40.91, 46.54, 56.00, 70.29, 70.48, 71.23, 77.21, 111.81, 112.43, 113.53, 114.00, 120.55, 121.90, 129.34, 130.41, 144.61, 146.03, 148.22, 148.58, 178.74; IR (neat): 1516 (C=C), 1767 (C=O), 3422 (OH) cm^{-1}; MS (EI) m/z 428 (M^+); HRMS (EI): calcd for $C_{25}H_{32}O_6$: 428.2199 (M^+), found: 428.2216; $[\alpha]_D^{25}$ −13.7 (c 0.70, $CHCl_3$).

*4.1.3.32. (3R,4R)-4-(4-Ethoxy-3-propoxybenzyl)-3-(4-hydroxy-3-propoxybenzyl)dihydrofuran-2-one (**4o**).* By the procedure similar to preparation of **4g**, **4o** was prepared from **14i** (63%) as a pale yellow oil: ^{1}H NMR (400 MHz, $CDCl_3$) δ: 1.02–1.07 (6H, m), 1.42 (3H, t, J = 7.1 Hz), 1.80–1.86 (4H, m), 2.41–2.63 (4H, m), 2.92 (2H, d, J = 5.9 Hz), 3.83–3.96 (5H, m), 4.01 (2H, q, J = 7.1 Hz), 4.07–4.11 (1H, m), 5.57 (1H, s), 6.51–6.84 (6H, m); ^{13}C NMR (100 MHz, $CDCl_3$) δ: 10.50, 22.59, 34.51, 38.05, 41.12, 46.48, 56.00, 65.22, 70.57, 71.40, 111.86, 112.79, 113.63, 114.72, 115.30, 119.36, 120.55, 121.40, 127.16, 127.28, 127.65, 128.36, 130.41, 131.16, 137.37, 147.43, 148.25, 148.58, 149.62, 178.7010.45, 14.87, 22.50, 22.60, 34.37, 38.04, 40.92, 46.58, 64,76, 70.33, 70.76, 71.26, 100.36, 112.48, 114.02, 114.06, 114.38, 129.37, 130.67, 144.63, 146.04, 147.70, 149.14; IR (neat): 1508 (C=C), 1770 (C=O) cm^{-1}; MS (EI) m/z 442 (M^+); HRMS (EI): calcd for $C_{26}H_{34}O_6$: 442.2355 (M^+), found: 442.2350; $[\alpha]_D^{25}$ −12.9 (c 0.50, $CHCl_3$).

*4.1.4. Effective synthesis of (3R,4R)-4-(3,4-diethoxybenzyl)-3-(4-hydroxy-3-ethoxybenzyl)dihydrofuran-2-one (**4m**)*

*4.1.4.1. 2-(3,4-Diehtoxybenzyl)malonic acid diethyl ester (**17**).* To a stirred solution of (3,4-diehtoxyphenyl)methanol (**16**) [16,23] (733 mg, 3.74 mmol) in CH_2Cl_2 (20 mL) were added NEt_3 (0.67 mL, 4.86 mmol) and MsCl (0.32 mL, 4.11 mmol) at 0 °C, and the reaction mixture was stirred at room temperature for 0.5 h. The reaction was quenched with sat. $NaHCO_3$ (aq) (10 mL), and the organic layer were separated. The aqueous layer was extracted with CH_2Cl_2 (20 mL × 3), and the organic layer and extracts were combined, dried over $MgSO_4$. The solvent was removed under reduced pressure to give a pale yellow oil, which was used directly in the next step. To a stirred solution of diethyl malonate (1.14 ml, 7.48 mmol) in DMF (20 mL) was added NaH (60%, 299 mg, 7.48 mmol) at 0 °C, and the resulting mixture was stirred at room temperature for 1 h. To the solution was added a solution of the oil obtained above in DMF (2 mL) at 0 °C, and the reaction mixture was stirred at room temperature for 25 h. The reaction was quenched with sat. $NaHCO_3$ (aq) (10 mL), and the aqueous mixture was extracted with Et_2O (20 mL × 3). The organic extracts were combined, dried over $MgSO_4$, evaporated to give a pale yellow oil which was chromatographed on silica gel (20 g, hexane:acetone = 15:1) to give **17** (1.10 g, 87% in 2 steps) as a pale yellow oil: ^{1}H NMR (300 MHz, $CDCl_3$) δ: 1.15–1.30 (6H, m), 1.39–1.46 (6H, m), 3.13 (2H, d, J = 8.0 Hz), 3.59 (1H, t, J = 8.0 Hz), 4.01–4.24 (8H, m), 6.68–6.78 (3H, m); ^{13}C NMR (75 MHz, $CDCl_3$) δ: 13.77, 13.83, 14.57, 14.60, 34.06, 41.37, 53.82, 61.11, 64.19, 113.33, 114.09, 120.83, 130.28, 147.28, 148.33, 166.34, 168.64; IR (neat): 1516 (C=C), 1731 (C=O) cm^{-1}; MS (EI) m/z 338 (M^+); HRMS (EI): calcd for $C_{23}H_{28}O_6$: 338.1729 (M^+), found: 338.1766.

*4.1.4.2. (R)-Acetic acid 3-(3,4-diethoxyphenyl-2-hydroxymethylpropyl ester (**18**).* To a stirred solution of **17** (1.43 g, 4.23 mmol) in THF (40 mL) was added $LiAlH_4$ (401 mg, 10.6 mmol) at 0 °C, and the resulting suspension was refluxed for 12 h. The reaction was quenched with 10% NaOH (aq) (20 mL), and the mixture was extracted with AcOEt (20 mL × 5). The organic extracts were combined dried over $MgSO_4$, and the solvent was evaporated to give diol, which was used directly in the next step. To a stirred solution of the diol obtained above in i-Pr_2O–THF (15 mL, 4:1) were added Lipase-PS (323 mg) and vinyl acetate (0.45 ml, 4.85 mmol), and the reaction mixture was stirred at room temperature for 2 h. The catalyst was filtered and the filtrate was evaporated to give residue, which was chromatographed on silica gel (30 g, hexane:acetone = 4:1) to give **18** (669 mg, 53% in 2 steps) as a pale yellow oil. The enantiomeric excess of **18** was determined to be a 98% ee by the Moscher's method [24]. ^{1}H NMR (300 MHz, $CDCl_3$) δ: 1.39–1.44 (6H, m), 2.06 (3H, s), 2.23 (1H, br), 2.49–2.64 (2H, m), 3.45–3.59 (2H, m), 4.01–4.08 (6H, m), 4.15 (1H, dd, J = 11.3, 4.7 Hz), 6.66–6.70 (2H, m), 6.78 (1H, d, J = 8.0 Hz); ^{13}C NMR (75 MHz, $CDCl_3$) δ: 14.88, 20.91, 33.86, 42.53, 62.07, 64.03, 64.55, 64.63, 113.69, 114.52, 121.22, 131.91, 147.23, 148.70, 171.68; IR (neat): 1513 (C=C), 1721 (C=O) cm^{-1}; MS (EI) m/z 296 (M^+); HRMS (EI): calcd for $C_{16}H_{24}O_5$: 296.1624 (M^+), found: 296.1594; $[\alpha]_D^{28}$ +18.8 (c 1.47, $CHCl_3$); 98% ee.

*4.1.4.3. (R)-Acetic acid 3-(3,4-Diethoxyphenyl-2-methanesulfonyloxymethylpropyl ester (**19**).* To a stirred solution of **18** (1.45 g, 4.96 mmol) in CH_2Cl_2 (25 mL) were added MsCl (0.42 ml, 5.45 mmol) and NEt_3 (0.89 ml, 6.45 mmol) at 0 °C, and the reaction mixture was stirred at room temperature for 0.5 h. The reaction was quenched with H_2O (20 mL), and the aqueous mixture was extracted with CH_2Cl_2 (20 mL × 3). The organic extracts were combined dried over $MgSO_4$, and evaporated. The residue was chromatographed on silica gel (40 g, hexane:acetone = 4:1) to give **19** (1.48 g, 79%) as a pale yellow oil: ^{1}H NMR (300 MHz, $CDCl_3$) δ: 1.41–1.46 (6H, m), 2.08 (3H, s), 2.32–2.36 (1H, m), 2.65 (2H, d, J = 7.4 Hz), 2.99 (3H, s), 4.00–4.23 (8H, m), 6.65–6.70 (2H, m), 6.80 (1H, d, J = 8.0 Hz); ^{13}C NMR (75 MHz, $CDCl_3$) δ: 14.85, 20.81, 30.90, 33.49, 37.21, 39.71, 63.02, 64.60, 68.48, 113.70, 114.40, 121.22, 130.36, 147.53, 148.82, 170.78; IR (neat): 1512 (C=C), 1735 (C=O) cm^{-1}; MS (EI) m/z 374 (M^+); HRMS (EI): calcd for $C_{17}H_{26}O_7S$: 374.1399 (M^+), found: 374.1362; $[\alpha]_D^{25}$ +2.1 (c 0.68, $CHCl_3$).

*4.1.4.4. (R)-4-(3,4-Diethoxybenzyl)dihydrofuran-2-one (**13d**) from **19**.* To a stirred solution of **19** (1.12 g, 3.00 mmol) in DMSO (25 mL) was added KCN (205 mg, 3.00 mmol), and the resulting mixture was heated at 90 °C for 3 h. After cooling, the reaction was quenched with H_2O (25 mL), and the aqueous mixture was extracted with Et_2O/AcOEt (1:1, 20 mL × 3). The organic extracts were combined, dried over $MgSO_4$, and evaporated to give cyanide, which was used directly in the next step. To a stirred solution of cyanide obtained above in THF–H_2O (3:1, 12 mL) was added $LiOH \cdot H_2O$ (126 mg, 3.00 mmol), and the reaction mixture was stirred at room temperature for 24 h. The reaction mixture was diluted with H_2O (10 mL), and the aqueous mixture was extracted with Et_2O (20 mL × 3). The organic extracts were combined, dried over $MgSO_4$, and evaporated to give alcohol, which was used directly in the next step. The alcohol obtained above was dissolved in 10% NaOH (aq) (15 mL), and the mixture was refluxed for 5 h. After cooling, 10% HCl (aq) (30 mL) and THF (30 mL) were added to

the reaction mixture, and the resulting solution was stirred at room temperature for 50 h. The aqueous reaction mixture was extracted with Et_2O (30 mL × 3), and the organic extracts were combined, dried over $MgSO_4$, and evaporated to give a residue, which was chromatographed on silica gel (30 g, hexane:acetone = 3:1) to give **13d** (475 mg, 60% in 3 steps) as a pale yellow oil.

4.2. In vitro preferential cytotoxicity

4.2.1. Cells and culture

Human pancreatic cancer cell lines, PANC-1 and CAPAN-1, were maintained in Dulbecco's modified Eagle's medium (DMEM, Nissui Pharmaceutical Co., Ltd., Tokyo, Japan) supplemented with 10% fetal bovine serum (FBS, Gibco BRL Products, Gaithersburg, MD, USA), 0.1% sodium bicarbonate (Nacalai Tesque Inc.), and 1% antibiotic-antimycotic solution (Sigma–Aldrich Inc., St. Louis, MO, USA). Nutrient deprived medium (NDM) contained 265 mg/L $CaCl_2 \cdot 2H_2O$, 0.1 mg/L $Fe(NO_3) \cdot 9H_2O$, 400 mg/L KCl, 200 mg/L $MgSO_4 \cdot 7H_2O$, 6400 mg/L NaCl, 700 mg/L $NaHCO_3$, 125 mg/L NaH_2PO_4, 15 mg/L phenol red, 1 M HEPES buffer (pH 7.4, Wako Pure Chemical Industries, Ltd., Osaka, Japan), and 10 mL MEM vitamin solution (Life Technologies, Inc., Rockville, MD, USA). The final pH was adjusted to 7.4 with 10% $NaHCO_3$. For amino acid supplementation, stock solutions (200 mmol/L L-glutamine solution, MEM amino acids solution, and MEM nonessential amino acids solution; Life Technologies) were added at a concentration of 1%.

4.2.2. Preferential cytotoxicity

Preferential cytotoxicity was determined as previously described [9]. In brief, PANC-1 or CAPAN-1 cells (2×10^4 cells/well) were seeded in 96-well plates (Corning Inc., Corning, NY, USA) and incubated in fresh DMEM at 37 °C under 5% CO_2 and 95% air for 24 h. The cells were washed with Dulbecco's phosphate-buffered saline (PBS, Nissui Pharmaceutical Co., Ltd., Tokyo, Japan) before the medium was replaced with either DMEM or NDM (for CAPAN-1, amino acids-supplimented NDM) containing serial dilutions of the test samples. After 24 h of incubation, the cells were washed with PBS, and 100 μL of DMEM containing 10% WST-8 cell counting kit solution (Dojindo, Kumamoto, Japan) was added to the wells. After 3 h of incubation, the absorbance was measured at 450 nm. Cell viability was calculated from the mean values for three wells using the following equation:

Cell viability (%) = [(Abs(test samples) − Abs(blank))/(Abs((control) − Abs(blank))] × 100

The preferential cytotoxicity was expressed as the concentration at which 50% of cells died preferentially in NDM (PC_{50}).

4.3. In vivo antitumor activity of triethoxy derivative **4m** in nude mice

Five-week-old female BALB/cAJcl-*nu/nu* mice were obtained from CLEA Japan, Inc. (Tokyo, Japan), and 5×10^6 CAPAN-1 cells in 0.3 mL DMEM were s.c. injected into the right side of the back of the animals. Two weeks later, 12 mice bearing tumors around 5 mm in diameter were randomly divided into treatment groups and a vehicle control group. Because (−)-arctigenin (**1**) and triethoxy derivative **4m** are poorly soluble in water, they were first dissolved in DMSO at 10 mg/mL and kept frozen until use. Just before administration, the stock solution was diluted in saline to a final concentration of 250 μg/mL (the final concentration of DMSO in saline is 2.5%). The mice were administered by *i.p.*-injections of 0.2 mL of solution of arctigenin, triethoxy derivative **4m**, or vehicle on 6 days of the week for 4 weeks. The tumor size and body weight were measured weekly and the tumor volume was calculated using the following formula: Tumor volume = $4/3 \times 3.14 \times (L/2 \times W/2 \times W/2)$ where L is the length of the tumor and W is its width. Results are expressed as means ±SD. Statistical comparisons were conducted using Student's t test after ANOVA. The results were considered to be significant when $P < 0.05$.

Acknowledgments

This work was supported in part by grants from the Ministry of Health and Welfare for the Third-Term Comprehensive 10-Year Strategy for Cancer Control and by Grant-in-Aid for Scientific Research (C) (No. 22590098) from Japan Society for the Promotion of Science (JSPS).

Appendix A. Supplementary data

Supplementary data related to this article can be found at http://dx.doi:10.1016/j.ejmech.2012.11.031H.

References

[1] J. Ferlay, H.R. Shin, F. Bray, D. Forman, C. Mathers, D.M. Parkin, GLOBOCAN 2008 v1.2, Cancer Incidence and Mortality Worldwide: IARC CancerBase No. 10 (Internet), International Agency for Research on Cancer, Lyon, France, 2010, Available from:, http://globocan.iarc.fr (accessed 08.05.12).
[2] D. Li, K. Xie, R. Wolff, J.L. Abbruzzese, Pancreatic cancer, Lancet 363 (2004) 1049–1057.
[3] S. Shore, D. Vimalachandran, M.G.T. Raraty, P. Ghaneh, Cancer in the elderly: pancreatic cancer, Surg. Oncol. 13 (2004) 201–210.
[4] H.W. Chung, S.M. Bang, S.W. Park, J.B. Chung, J.K. Kang, J.W. Kim, J.S. Seong, W.J. Lee, S.Y. Song, A prospective randomized study of gemcitabine with doxifluridine versus pacritaxel with doxifluridine in concurrent chemo-radiotherapy for locally advanced pancreatic cancer, Int. J. Radiat. Oncol. 60 (2004) 1494–1501.
[5] C.V. Dang, G.L. Semenza, Oncogenic alteration of metabolism, Trends Biochem. Sci. 24 (1999) 68–72.
[6] M. Kitano, M. Kudo, K. Maekawa, Y. Suetomi, H. Sakamoto, N. Fukuta, R. Nakaoka, T. Kawasaki, Dynamic imaging of pancreatic diseases by contrast enhanced coded phase inversion harmonic ultrasonography, Gut 53 (2004) 854–859.
[7] K. Izuishi, K. Kato, T. Ogura, T. Kinoshita, H. Esumi, Remarkable tolerance of tumor cells to nutrient deprivation: possible new biochemical target for cancer therapy, Cancer Res. 60 (2000) 6201–6207.
[8] (a) H. Esumi, J. Lu, Y. Kurashima, T. Hanaoka, Antitumor activity of pyrvinium pamoate, 6-(dimethylamino)-2-[2-(2,5-dimethyl-1-phenyl-1*H*-pyrrol-3-yl) ethenyl]-1-methyl-quinolinium pamoate salt, showing preferential cytotoxicity during glucose starvation, Cancer Sci. 95 (2004) 685–690;
(b) J. Lu, S. Kunimoto, Y. Yamazaki, M. Kaminishi, H. Esumi, D. Kigamicin, A novel anticancer agent based on a new anti-austerity strategy targeting cancer cells' tolerance to nutrient starvation, Cancer Sci. 95 (2004) 547–552.
[9] S. Awale, J. Lu, S.K. Kalauni, Y. Kurashima, Y. Tezuka, S. Kadota, H. Esumi, Identification of arctigenin as an antitumor agent having the ability to eliminate the tolerance of cancer cells to nutrient starvation, Cancer Res. 66 (2006) 1751–1757.
[10] (a) B. Hausott, H. Greger, B. Marian, Naturally occurring lignans efficiently induce apoptosis in colorectal tumor cells, J. Cancer Res. Clin. Oncol. 129 (2003) 569–576;
(b) T. Matsumoto, K. Hosono-Nishiyama, H. Yamada, Antiproliferative and apoptotic effects of butyrolactone lignans from *Arctium lappa* on leukemic cells, Planta Med. 72 (2006) 276–278;
(c) T. Toyoda, T. Tsukamoto, T. Mizoshita, S. Nishibe, T. Deyama, Y. Takenaka, N. Hirano, H. Tanaka, S. Takasu, H. Ban, T. Kumagai, K. Inada, H. Utsunomiya, M. Tatematsu, Inhibitory effect of nordihydroguaiaretic acid, a plant lignan, on *Helicobacter pylori*-associated gastric carcinogenesis in Mongolian gerbils, Cancer Sci. 98 (2007) 1689–1695.
[11] (a) M. Nose, T. Fujimoto, T. Takeda, S. Nishibe, Y. Ogihara, Structural transformation of lignan compounds in rat gastrointestinal tract, Planta Med. 58 (1992) 520–523;
(b) S. Heinonen, T. Nurmi, K. Liukkonen, K. Poutanen, K. Wähälä, T. Deyama, S. Nishibe, H. Adlercreuta, In vitro metabolism of plant lignans: new precursors of mammalian lignans enterolactone and enterodiol, J. Agr. Food Chem. 49 (2001) 3178–3186;
(c) L.-H. Xie, E.-M. Ahn, T. Akao, A.A. Abdel-Hafez, N. Nakamura, M. Hattori, Transformation of arctiin to estrogenic and antiestrogenic substances by human intestinal bacteria, Chem. Pharm. Bull. 51 (2003) 378–384.
[12] E. Eich, H. Pertz, M. Kaloga, J. Schulz, M.R. Fesen, A. Mazumder, Y. Pommier, (−)-Arctigenin as a lead structure for inhibitors of human immunodeficiency virus type-1 integrase, J. Med. Chem. 39 (1996) 86–95.
[13] M.G. Banwell, S. Chand, G.P. Savage, An enantioselective total synthesis of the stilbenolignan (−)-aiphanol and the determination of its absolute stereochemistry, Tetrahedron: Asymmetry 16 (2005) 1645–1654.

[14] R. Fumeaux, C. Menozzi-Smarrito, A. Stalmach, C. Munari, K. Kraehenbuehl, H. Steiling, A. Crozier, G. Williamson, D. Barron, First synthesis, characterization, and evidence for the presence of hydroxycinnamic acid sulfate and glucuronide conjugates in human biological fluids as a result of coffee consumption, Org. Biomol. Chem. 8 (2010) 5199–5211.
[15] T. Cardinaels, J. Ramaekers, P. Nockemann, K. Driesen, K. Van Hecke, L. Van Meervelt, S. Lei, S. De Feyter, D. Guillon, B. Donnio, K. Binnemans, Imidazo[4,5-f]-1,10-phenanthrolines: versatile ligands for the design of metallomesogens, Chem. Mater. 20 (2008) 1278–1291.
[16] T.C. Daniels, R.E. Lyons, Ethyl esters of triiodophenoxyacetic acids and potassium triiodophenoxyacetate, J. Am. Chem. Soc. 58 (1936) 2646.
[17] M. Lieber, J. Mazzetta, W. Nelson-Rees, M. Kaplan, G. Todaro, Establishment of a continuous tumor-cell line (PANC-1) from a human carcinoma of the exocrine pancreas, Int. J. Cancer 15 (1975) 741–747.
[18] (a) H. Suemizu, M. Monnai, Y. Ohnishi, M. Ito, N. Tamaoki, M. Nakamura, Identification of a key molecular regulator of liver metastasis in human pancreatic carcinoma using a novel quantitative model of metastasis in NOD/SCID/γ_c^{null} (NOG) mice, Int. J. Oncol. 31 (2007) 741–751;
(b) A.P. Kyriazis, A.A. Kyriazis, D.G. Scarpelli, J. Fogh, M.S. Rao, R. Lepera, Human pancreatic adenocarcinoma line Capan-1 in tissue culture and the nude mouse. Morphologic, biologic, and biochemical characteristics, Am. J. Pathol. 106 (1982) 250–260.
[19] S. Koul, B. Singh, S.C. Taneja, G.N. Qazi, New chemo and chemo-enzymatic synthesis of β-benzyl-γ-butyrolactones, Tetrahedron 59 (2003) 3487–3491.
[20] A. Van Oeveren, J.F.G.A. Jansen, B.L. Feringa, Enantioselective synthesis of natural dibenzylbutyrolactone lignans (−)-enterolactone, (−)-hinokinin, (−)-pluviatolide, (−)-enterodiol, and furofuran lignan (−)-eudesmin via tandem conjugate addition tp g-alkoxybutenolides, J. Org. Chem. 59 (1994) 5999–6007.
[21] Aurora Building Blocks, Order Number: A00. 384. 218.
[22] B. Pelcman, J.G.K. Yee, L.F. Macenzie, Y. Zhou, K. Han, Isochromenones as PDE4 and PDE7 inhibitors and their preparation and use in the treatment of inflammation, PCT Int. Appl., 2010076564, 2010.
[23] (a) A. Enoki, M.H. Gold, Degradation of the diarylpropane lignin model compound 1-(3′,4′-diethoxyphenyl)-l,3-dihydroxy-2-(4‴-methoxyphenyl)-propane and derivatives by the basidiomycete *Phanerochaete chrysosporium*, Arch. Microbiol. 132 (1982) 123–130;
(b) V.C. Farmer, M.E.K. Henderson, J.D. Russel, Reduction of certain aromatic acids to aldehydes and alcohols by *Polystictus versicolor*, Biochim. Biophys. Acta 35 (1959) 202–211.
[24] J.A. Dale, S.H. Mosher, Nuclear magnetic resonance enantiomer regents. Configurational correlations via nuclear magnetic resonance chemical shifts of diastereomeric mandelate, *O*-methylmandelate, and α-methoxy-α-trifluoromethylphenylacetate (MTPA) esters, J. Am. Chem. Soc. 95 (1973) 512–519.

OPEN ACCESS Freely available online

PLOS ONE

Critical Role of H_2O_2 Generated by NOX4 during Cellular Response under Glucose Deprivation

Satoshi Owada[1,2], Yuko Shimoda[1,2], Katsuya Tsuchihara[1,2], Hiroyasu Esumi[1,2]*

1 Department of Integrated Biosciences, Graduate School of Frontier Sciences, The University of Tokyo, Kashiwa, Japan, 2 Cancer Physiology Project, Research Center for Innovative Oncology, National Cancer Center Hospital East, Kashiwa, Japan

Abstract

Glucose is the most efficient energy source, and various cancer cells depend on glycolysis for energy production. For maintenance of survival and proliferation, glucose sensing and adaptation to poor nutritional circumstances must be well organized in cancer cells. While the glucose sensing machinery has been well studied in yeasts, the molecular mechanism of glucose sensing in mammalian cells remains to be elucidated. We have reported glucose deprivation rapidly induces AKT phosphorylation through PI3K activation. We assumed that regulation of AKT is relevant to glucose sensing and further investigated the underlying mechanisms. In this study, AKT phosphorylation under glucose deprivation was inhibited by galactose and fructose, but induced by 2-deoxyglucose (2-DG). Both 2-DG treatment and glucose deprivation were found to induce AKT phosphorylation in HepG2 cells. These findings suggested that glucose transporter may not be involved in the sensing of glucose and induction of AKT phosphorylation, and that downstream metabolic events may have important roles. A variety of metabolic stresses reportedly induce the production of reactive oxygen species (ROS). In the present study, glucose deprivation was found to induce intracellular hydrogen peroxide (H_2O_2) production in HepG2 cells. N-acetylcysteine (NAC), an antioxidant reagent, reduced both the increase in cellular H_2O_2 levels and AKT phosphorylation induced by glucose deprivation. These results strongly suggest that the glucose deprivation-induced increase of H_2O_2 in the cells mediated the AKT phosphorylation. RNA interference of NOX4, but not of NOX5, completely suppressed the glucose deprivation-induced AKT phosphorylation as well as increase of the intracellular levels of ROS, whereas exogenous H_2O_2 could still induce AKT phosphorylation in the NOX4-knockdown cells. In this study, we demonstrated that the ROS generated by NOX4 are involved in the intracellular adaptive responses by recognizing metabolic flux.

Citation: Owada S, Shimoda Y, Tsuchihara K, Esumi H (2013) Critical Role of H_2O_2 Generated by NOX4 during Cellular Response under Glucose Deprivation. PLoS ONE 8(3): e56628. doi:10.1371/journal.pone.0056628

Editor: Junji Yodoi, Institute for Virus Research, Laboratory of Infection and Prevention, Japan

Received October 1, 2012; **Accepted** January 11, 2013; **Published** March 21, 2013

Funding: This work was supported by a Grant for the 3rd Term Comprehensive 10-Year Strategy for Cancer Control from the Ministry of Health, Labour and Welfare Japan [H22-3ji taigann-ippann-033 to HE] (http://www.mhlw.go.jp/english/). No additional external funding received for this study. The funders had no role in study design, data collection and analysis, decision to publish, or preparation of the manuscript.

Competing Interests: The authors have declared that no competing interests exist.

* E-mail: hesumi@ncc.go.jp

Introduction

The supply of nutrients and oxygen is pivotal for cell survival and function, because of the large energy requirements of cells. This need is especially critical during cell proliferation. Proliferation is a process during which the numbers of cells successively double; therefore, the synthesis of nucleic acids, lipids, proteins and sugars is obligatory for successful proliferation. Glucose serves as a carbon source for the synthesis of nucleic acids, non-essential amino acids, lipids, and sugar. The intermediate metabolites in the glycolytic system are indispensable for non-essential amino acid synthesis, and intermediate metabolites and coenzymes in the pentose-5-phosphate pathway are required for the synthesis of nucleic acids and lipids. In addition, glucose is also needed for energy production in all cells.

Because of the pivotal role of glucose in the maintenance of the cellular functions, survival, and proliferation, elaborate mechanisms for detecting glucose availability in the cellular microenvironment exist in cells. The molecular mechanisms involved in the sensing of extracellular glucose concentrations have been extensively studied in yeasts. Yeasts detect the extracellular glucose concentrations using Snf3/Rtg2 (a glucose transporter homolog that has no capability as a transporter). Extracellular glucose causes this sensor to generate an intracellular signal that induces the expressions of several HXT genes encoding hexose transporters. The glucose signal induces HXT gene expression by influencing the function of the Rgt1 transcriptional repressor. In the absence of glucose, Rgt1 is functional and binds to the promoters of the HXT genes, repressing their functions [1,2,3]. In contrast, the biochemical basis of the glucose sensing mechanism in mammalian cells is largely unknown.

Meanwhile, most of human cancer tissues are known to be hypoxic, the hypoxia being caused mainly by a poor and heterogeneous blood supply [4,5,6,7]. Glucose as well as oxygen is supplied to cancer tissues via the blood stream, and we assumed that the glucose supply might be limited in human cancer tissues. In fact, the glucose concentrations in human colon cancer and gastric cancer tissues were found to be significantly lower than those in surrounding non-cancerous tissues [8]. In the cancer cells that exist in such environments, the monitoring of and adaptation to extracellular glucose concentrations are assumed to be important for the survival/proliferation of the tumor cells. We previously reported that AKT phosphorylation is immediately enhanced by the absence of glucose and plays a critical role in

cellular survival under such condition in various cell lines [9,10]. AKT can also be activated in response to a variety of cellular stresses, such as heat shock, ultraviolet light irradiation, ischemia, hypoxia, hyperglycemia, and oxidative stress. AKT is a serine and threonine kinase that mediates cell survival under these aforementioned conditions [11,12,13,14,15].

In the present study, we attempted to elucidate the molecular and biochemical mechanisms involved in the sensing of mammalian cells of the extracellular glucose concentrations, using AKT phosphorylation as an index of the cellular responses to glucose deprivation. We demonstrate the contribution of the H_2O_2 generated by NOX4 in the cellular sensing of and adaptation to poor glucose supply.

Materials and Methods

Cell cultures

Human fibroblasts derived from the subserosa of the stomach used for this study were kindly gifted to us by Dr Atsushi Ochiai (Pathology Division, Research Center for Innovative Oncology, National Cancer Center Hospital East). Human pancreatic cancer cells (PANC-1), human hepatocellular carcinoma cells (HepG2) and human fibroblasts derived from subserosa of the stomach were cultured in DMEM (GIBCO) supplemented with 10% fetal bovine serum (Biowest). All the cells were purchased from ATCC. The glucose-deprived condition was created as described previously [16].

Reagents

2′, 7′- Dichlorodihydrofluorescin diacetate (DCFDA) was purchased from Invitrogen. 3′-O-Acetyl-6′-O-pentafluorobenzenesulfonyl-2′,7′-difluorofluorescein (Bes-H_2O_2), galactose and fructose were purchased from Wako Pure Chemical Industries. N-acetyl-L-cysteine (NAC) and 2-deoxy-D-glucose (2-DG) were purchased from Sigma Aldrich. LY294002 and PP2 were purchased from Calbiochem.

Immunoblot analyses

Cells were homogenized in lysis buffer containing 10% SDS (sodium dodecyl sulfate), 10 mM Tris-HCl (pH 7.5) and 1 mM sodium orthovanadate, as described previously [17], and subjected to SDS-PAGE (SDS polyaclylamide gel electrophoresis). The proteins were transferred to a polyvinylidene fluoride microporous membrane (Millipore). The primary antibodies used were: anti-phospho-AKT Ser-473, anti-phospho-SRC Family Tyr-416, and anti-AKT, all obtained from Cell Signaling Technologies, and anti-actin (sc-1615), and c-SRC antibody (SRC2), obtained from Santa Cruz Biotechnology. The anti-OSSA antibody was a kind gift from Dr. Ryuuichi Sakai, National Cancer Center Research Institute. The following secondary antibodies were purchased from Santa Cruz Biotechnology: goat anti-mouse IgG-HRP, goat anti-rabbit IgG-HRP. The immunoblots were scanned using a CanoScan LiDE60 image scanner (Canon).

siRNA transfection

OSSA, NOX4, NOX5, and non-targeting siRNA were purchased from Invitrogen. For the siRNA experiments, the cells were transfected separately using a non-targeting siRNA or two separate specific siRNAs using Lipofectamine 2000 (Invitrogen).

RT-PCR

Total RNAs were prepared from the cells using ISOGEN (Nippon Gene), and reverse transcription was performed using superscript VILO (Invitrogen). PCR for human NOX family genes was carried out using the following primers: forward 5′-CTCAGCGGAATCAATCAGCTGTG-3′ and reverse 5′-AGAGGAACACGACAATCAGCCTTAG-3′ for Nox4; forward 5′-ATCAAGCGGCCCCCTTTTTTTCAC-3′ and reverse 5′-CTCATTGTCACACTCCTCGACAGC-3′ for Nox5.

Measurement of intracellular ROS levels

The cells were treated under various conditions and then incubated in DMEM or glucose-deprived medium containing 5 μM of DCFDA or 5 μM BES-H_2O_2-Ac at 37°C for 30 min. Then, the cells were detached from the plate with trypsin/EDTA, washed with PBS, resuspended in 500 μL of PBS, and placed on ice, protected from light. The intensity of the fluorescence of each cell was immediately measured using a FACS CANTO (Becton Dickinson) equipped with an argon ion laser (488 nm excitation). Each experiment was conducted in triplicate, and 10,000 cells per sample were measured. The histogram was analyzed using the software program BD FACS DIVA (Becton Dickinson).

Results

AKT activation by glucose deprivation

Within 30 minutes, and still after 3 hours, of transferring the HepG2 cells from ordinary DMEM to glucose-deprived medium, AKT was strongly phosphorylated at Ser 473; furthermore, AKT phosphorylation was significantly inhibited by treatment with LY294002 [18], an inhibitor of PI3K (Fig. 1A). Similarly, PI3K-dependent AKT activation was also observed in the pancreatic PANC-1 cells (Fig. S1) in a previous study [10]. Furthermore, increase of AKT phosphorylation induced by glucose deprivation was also observed in human fibroblasts derived from the subserosa of the stomach (Fig. S2).

To examine how glucose deprivation is recognized in these cells, concentration-dependent AKT activation in response to glucose deprivation was examined. When the HepG2 cells were exposed to media containing less than 1.38 mM of glucose, corresponding to one-quarter of the blood glucose level, AKT activation was clearly observed (Fig. 1B). Similarly, an increase in AKT phosphorylation was also observed in PANC-1 cells cultured in the presence of glucose at concentrations of less than 0.69 mM (Fig. S3). To elucidate the glucose sensing mechanism of the cells, the effect of glucose analogues on the AKT activation in response to glucose deprivation was examined. AKT activation was completely inhibited by the addition of either galactose or fructose at a final concentration of 5.5 mM (Fig. 1C). Similar results were observed in the PANC-1 cells (Fig. S4). These observations indicate that AKT is activated by a decrease of some metabolites of glycolysis or metabolic stress, rather than by the decrease of glucose itself. In yeast, the extracellular glucose concentration is sensed by a glucose transporter [1,2,3]. To examine whether a similar mechanism may also prevail in mammalian cells, the influence of 2-DG [19,20] on the AKT phosphorylation induced by glucose deprivation was examined. As shown in Fig. 1D, AKT phosphorylation in the HepG2 cells in response to glucose deprivation was not inhibited by 2-DG. Rather, AKT phosphorylation was clearly induced by the addition of 5.5 mM 2-DG, even in the presence of glucose. This observation indicates that glucose is not sensed by binding to a receptor or transporter, nor is it sensed by hexokinase, because 2-DG can be phosphorylated as efficiently by mammalian hexokinase as glucose. It is possible that the inhibition of binding of some sensors to glucose, if such an interaction occurs, might evoke the same cellular responses as glucose deprivation.

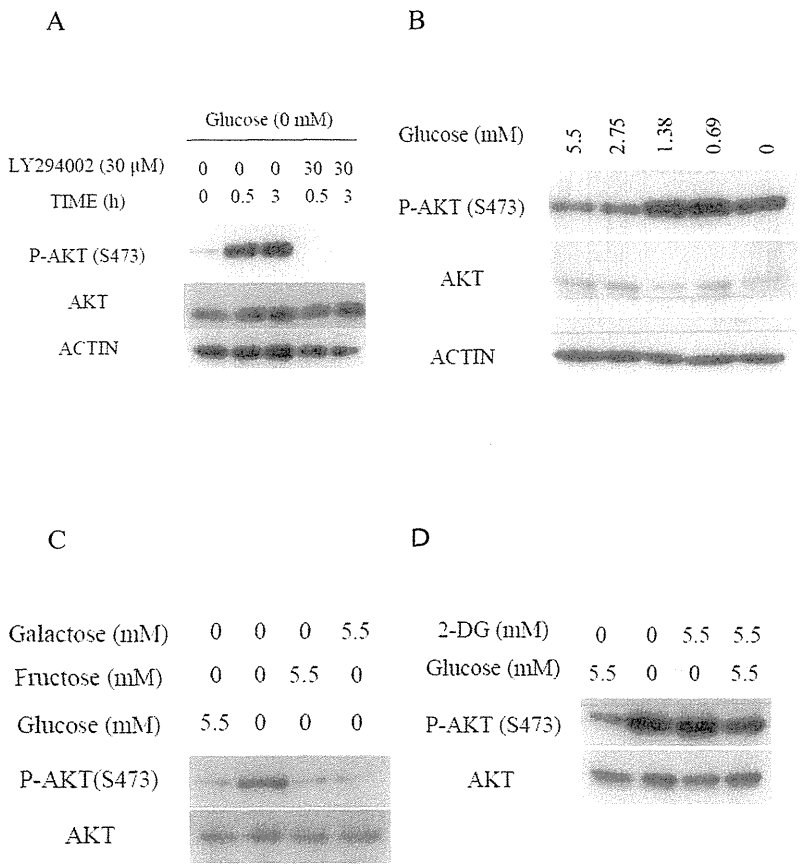

Figure 1. AKT phosphorylation was induced under glucose deprivation. (A) Immunoblotting analyses after incubation of HepG2 cells in the absence or presence of 5.5 mM of glucose and absence or presence of 30 μM of LY294002 for the indicated times. (B) HepG2 cells treated or not treated with various concentrations of glucose for 0.5 h were subjected to immunoblotting. (C) Immunoblotting analyses of HepG2 cells treated or not treated with 5.5 mM of glucose, 5.5 mM of galactose, or 5.5 mM of fructose for 0.5 h. (D) Immunoblotting analyses of HepG2 cells treated or not treated with 5.5 mM of glucose, 5.5 mM of 2-DG, or 5.5 mM of glucose plus 5.5 mM of 2-DG for 0.5 h.
doi:10.1371/journal.pone.0056628.g001

Role of hydrogen peroxide in the activation of AKT in response to glucose deprivation

Since AKT phosphorylation in response to glucose deprivation was attenuated by galactose, we assumed that changes in the metabolism might be the cause of the increase in AKT activation. Reactive oxygen species (ROS) are reportedly produced in cells under metabolic stresses [21,22]. We evaluated the intracellular levels of ROS using dichlorofluorescein diacetate (DCFDA), which measures hydroxyl and peroxyl radicals and other ROS. A significant increase in the intracellular ROS production was observed in the HepG2 cells cultured in glucose-deprived medium treated with DCFDA for 30 minutes (Fig. 2A). 3′-O-acetyl-6′-O-pentafluorobenzenesulfonyl- 2′,7′-difluorofluorescein (BES-H_2O_2) specifically detects an increase in the amounts of hydrogen peroxide (H_2O_2) [23] in cells treated under the same conditions (Fig. 2B). An increase in the production of ROS induced by glucose deprivation was also observed in the PANC-1 cells and human fibroblasts derived from the subserosa of the stomach (Fig. S5,S6). Addition of galactose or fructose completely prevented the H_2O_2 increase (Fig. S7). These results clearly showed that H_2O_2 production is induced by glucose deprivation. To elucidate the causal relationship between H_2O_2 production and AKT phosphorylation, the effect of addition of exogenous H_2O_2 on AKT phosphorylation was examined. Exogenous H_2O_2 addition to the culture medium induced PI3K-dependent AKT phosphorylation in a manner similar to glucose deprivation (Fig. 2C). To confirm the causal relation further, the influence of N-acetylcysteine (NAC), an antioxidant reagent, on the AKT phosphorylation induced in the absence of glucose was examined. The addition of NAC to the culture medium at a final concentration of 12.5 mM markedly reduced the ROS levels even under glucose-deprived conditions (Fig. 2A and 2B). Furthermore, the NAC treatment also suppressed the AKT phosphorylation induced by glucose deprivation (Fig. 2D).

SRC and OSSA are indispensable for AKT phosphorylation induced by glucose deprivation

SRC is involved in an alternate PI3K-activating pathway, and OSSA, a scaffold protein also known as FAM120A, reportedly activates the SRC-PI3K pathway in the presence of oxidative stress [24]. Thus, the involvements of SRC and OSSA in the glucose deprivation-induced phosphorylation of AKT were examined. PP2, a specific SRC family inhibitor [25], clearly inhibited the AKT phosphorylation induced by glucose deprivation (Fig. 3A). PP2 also inhibited AKT phosphorylation induced by exogenous H_2O_2 (Fig. 3B). Consistent with these findings, PP2

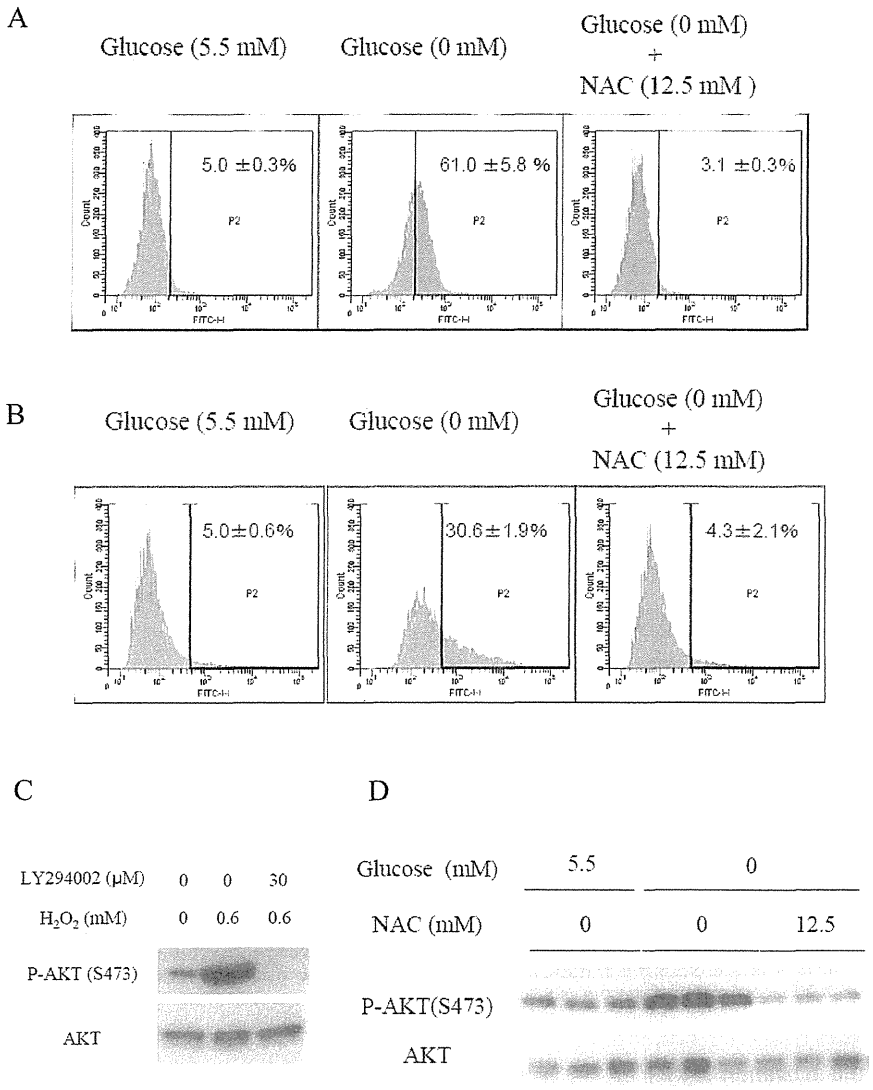

Figure 2. ROS mediates AKT phosphorylation under glucose deprivation. (A)(B)(D) HepG2 cells were cultured in either glucose-containing medium or glucose-deprived medium in the absence or presence of 12.5 mM of NAC for 0.5 h. ROS production was measured using flow cytometry. Cells were stained with (A) 5 μM of DCFDA or (B) 5 μM of BES-H_2O_2. Cells were gated within a range contained in the upper 5% of the total cell count under the glucose replete condition. (D) The AKT phosphorylation level was evaluated by immunoblotting. (C) Addition of H_2O_2 to media containing 5.5 mM of glucose in the absence or presence of 30 μM of LY294002 for 0.5 h, followed by immunoblotting.
doi:10.1371/journal.pone.0056628.g002

also suppressed the phosphorylation of SRC induced by glucose deprivation and exogenous H_2O_2 (Fig. S8). PP2 treatment did not alter the increased ROS levels in HepG2 cells cultured under glucose-deprived conditions (Fig. 3C). Similarly, LY294002 treatment inhibited AKT phosphorylation, but did not alter the ROS production (Fig. 1A, 3C). Suppression of OSSA expression by RNA interference inhibited the AKT phosphorylation induced by glucose deprivation and exogenous H_2O_2 (Fig. 3D, 3E and 3F). Thus, SRC and OSSA were concluded as being mediators of the H_2O_2 signals induced by glucose deprivation that activate the PI3K-AKT axis.

NOX4 knockdown inhibits hydrogen peroxide generation under glucose-deprived conditions

NOX4, one of the members of the NADPH oxidase family, is known to be closely involved in the production of ROS in response to growth factor stimuli [26]. Thus, its involvement also in glucose deprivation-induced AKT phosphorylation was examined. RNA interference selectively reduced the expression of NOX4 in HepG2 cells (Fig. 4A). Increase of intracellular ROS levels by glucose deprivation was suppressed by NOX4 knockdown (Fig. 4B). Consistent with this finding, AKT phosphorylation was also not induced in the NOX4 knockdown cells, while exogenous H_2O_2 clearly induced AKT phosphorylation in the cells (Fig. 4C). Similar results were obtained in the PANC-1 cells (Fig. S9A, B). PANC-1 cells express NOX5 as well as NOX4, however,

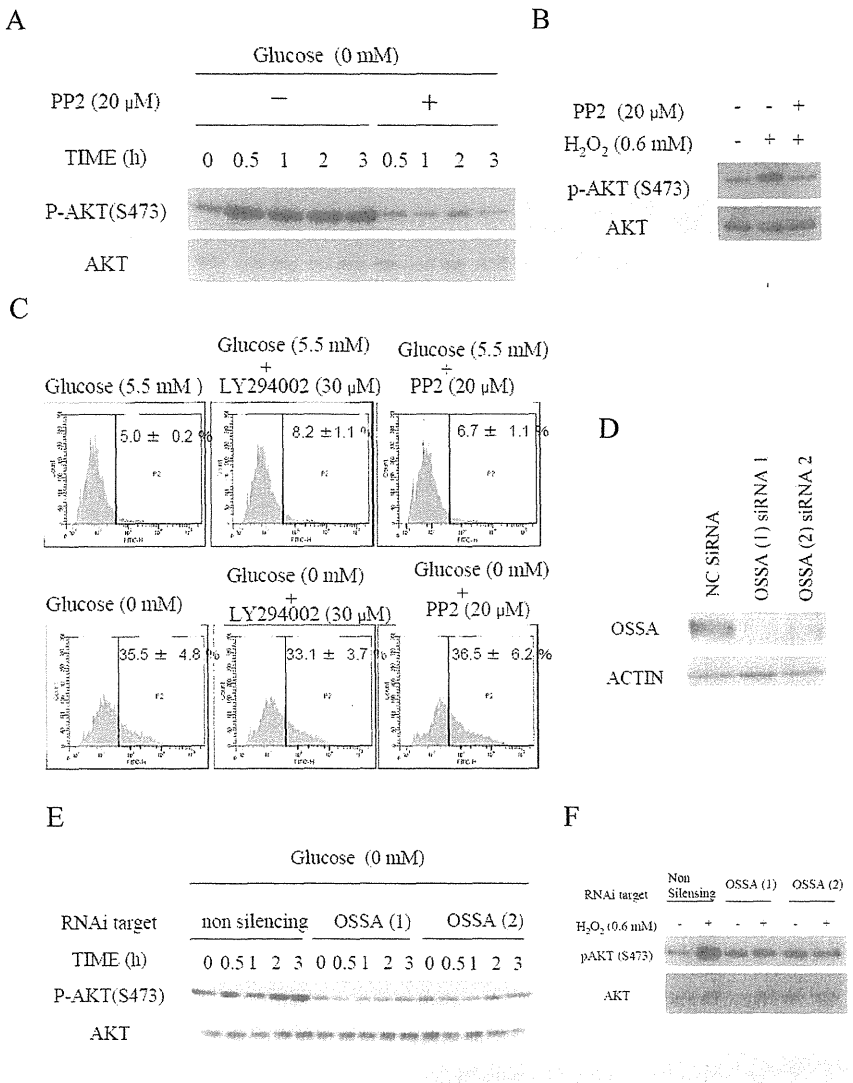

Figure 3. SRC and OSSA are indispensable for the AKT phosphorylation induced by glucose deprivation. (A) Immunoblotting analyses of HepG2 cells in the absence or presence of 5.5 mM of glucose in the and absence or presence of 20 μM of PP2 for the indicated times. (B) Addition of H_2O_2 to the culture medium containing 5.5 mM glucosein the absence or presence of 20 μM of PP2 for 0.5 h, followed by immunoblotting. (C) HepG2 cells were cultured in medium containing or not containing (glucose-deprived) 5.5 mM of glucose in the absence or presence of 30 μM of LY204002 or 20 μM of PP2 for 0.5 h. The cells were stained with 5 μM of BES-H_2O_2. ROS production was measured using flow cytometry. (D) siRNA-treated HepG2 cells were subjected to immunoblotting analyses using OSSA antibody. (E) Immunoblotting analyses of HepG2 cells transfected with a non-targeting siRNA or two separate OSSA siRNAs in the absence or presence of 5.5 mM of glucose for the indicated times. (F) Addition of H_2O_2 to the medium of OSSA-knockdown cells containing 5.5 mM glucose for 0.5 h, followed by immunoblotting.
doi:10.1371/journal.pone.0056628.g003

knockdown of NOX5 did not alter the AKT phosphorylation level (Fig. S10A, B).

Discussion

In this study, we tried to elucidate the mechanism of sensing of the extracellular glucose concentration by cells, using AKT phosphorylation as a marker. As reported previously, AKT phosphorylation is induced by glucose deprivation [9,10]. In addition, increase in AKT phosphorylation has also been confirmed in HepG2 cells cultured in media containing one-quarter of the normal physiological glucose concentration. This fact suggests that cells have sophisticated mechanisms for monitoring extracellular glucose levels. In another study, increase in AKT phosphorylation was confirmed in PANC-1 cells cultured in the presence of glucose levels that are one-eighth of the normal physiological condition. The difference in the minimal trigger concentration of glucose between the HepG2 cells and PANC-1 cells could be related to differences in the origins of the cells or differences in the microenvironments of the tumors the cells were derived from.

In the present study, increase in ROS production was observed by 30 minutes after glucose deprivation, both in cancer cells and human fibroblasts. Thus, it became evident that the mechanism of ROS production under glucose deprivation is preserved in not only cancer cells, but also human fibroblasts. ROS was strongly suspected to mediate the AKT phosphorylation, because AKT